5.RESULTS

5.1 Expression profiling of TLRs 1, 2, 3, 4, 5, 6, 7, 8, 9, 10 on HNSCC cell line

The mRNA-based expression of TLRs 1-10 in HEp-2 cells was quantitated by qPCR. Considering average $C_t \leq 35$ for the presence of the particular mRNA, all the TLRs were found expressed in HEp-2, except TLR-2 and TLR-10. TLR-7 was minimally expressed while TLR-4 mRNA was most prominently expressed in HEp-2. The average C_t values of TLRs are represented in the **Figure 5.1.**

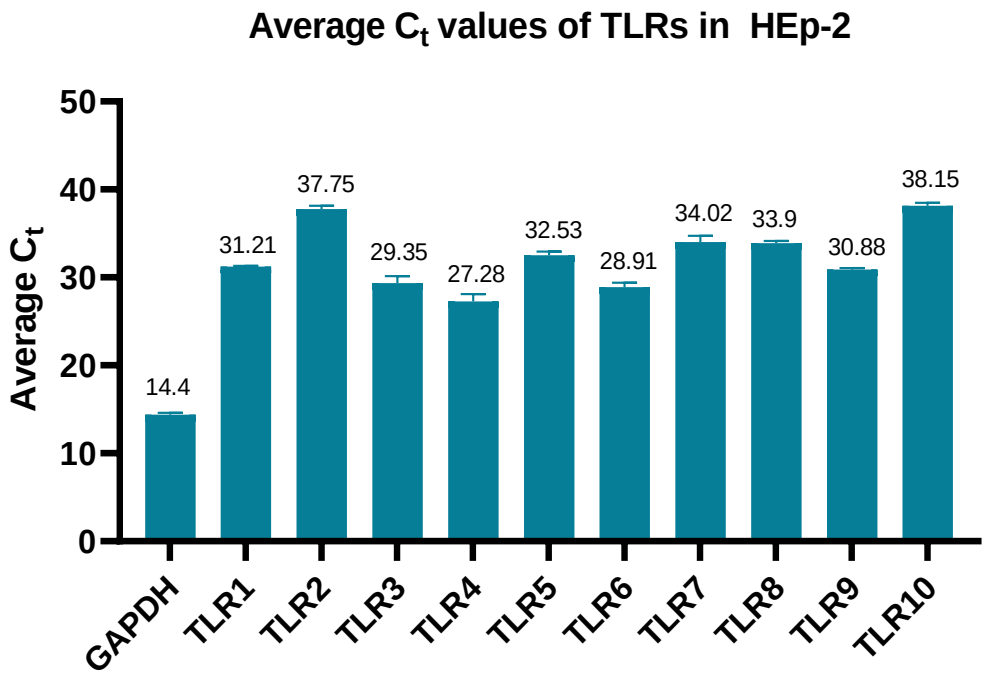

Figure 5.1: Expression of TLRs in HNSCC cell line HEp-2. Bar graph of average C_t values of TLRs in HEp-2 determined by qPCR.

5.2 Evaluation of constitutive TLR signaling in HNSCC cell line

To examine whether the constitutive TLR signaling is ongoing in HEp-2, status of the phosphorylated forms of downstream kinases IRAK-1 and IRAK-4 was used as a marker. Total and phosphorylated IRAK-1 and IRAK-4 levels were estimated by intracellular cytokines staining method followed by flow cytometry.

Figure 5.2 A & B shows representative histogram images for expression of IRAK-1, IRAK-4 and their phosphorylated forms in HEp-2. 15.4 ± 2.9% of total HEp-2 cells were IRAK-1+ of which 9.6 ± 1.8% were phosphorylated while maintaining the equivalent MFI. This data indicated that 62% of IRAK-1+ cells existed in their activated state **(Figure 5.2 C & D)**. Further, 9.8 ± 1.7% of total HEp-2 cells were IRAK-4+ of which 9.3 ± 1.7% were phosphorylated while maintaining the equivalent MFI. This data indicated that 92% of IRAK-4+ cells existed in their activated state **(Figure 5.2 C & D)**.

The results suggested that IRAK dependent TLR signaling is constitutively on in HEp-2 cells.

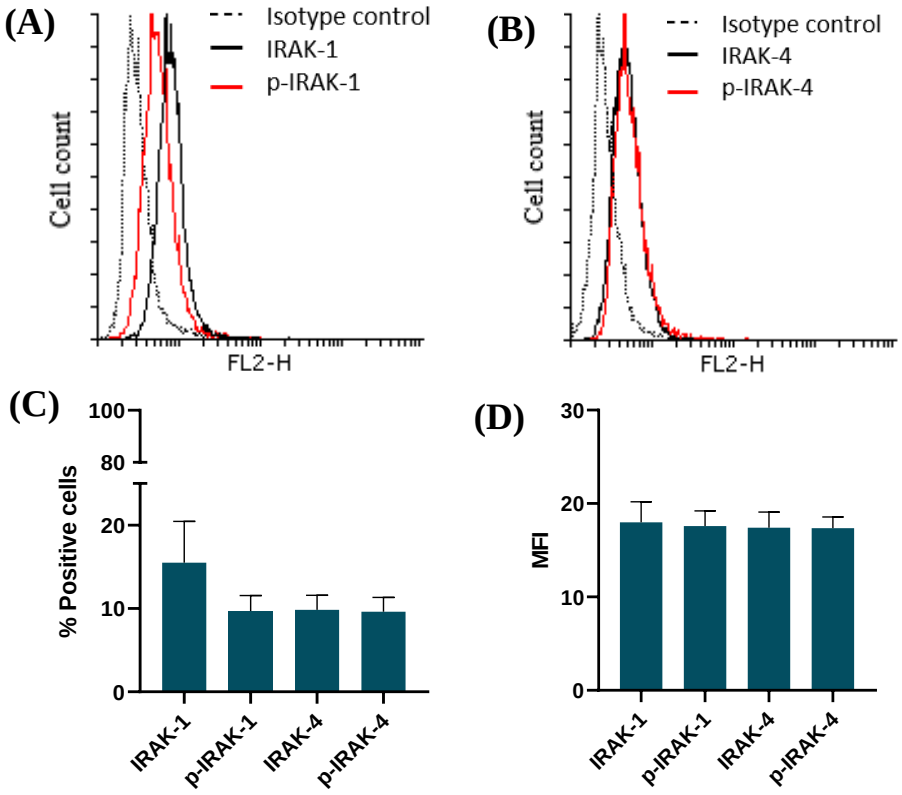

Figure 5.2: Evaluation of IRAKs and their phosphorylated forms in HNSCC cell line HEp-2.
(A) Representative histogram image of expression of IRAK-1 and its phosphorylated forms in HEp-2. (B) Representative histogram image of expression of IRAK-4 and its phosphorylated forms in HEp-2. Bar graphs of (B) percent positive cells and (C) MFI of IRAKs and their phosphorylated forms. Data from three independent experiments is summarized and presented as mean ± S.D.

5.3 Evaluation of the impact of TLR signaling on the oncogenic properties of HNSCC cell line

Following markers associated with features like survival, proliferation, cancer stem cells (CSCs) formation, metastasis and EMT were selected to characterize the pro-oncogenic properties of HNSCC cells.

- Cell survival- Bcl-2 and Bcl-xL
- Proliferative potential- Ki-67
- Cancer stem cell (CSCs) formation- CD44, Nanog and ALDH1
- EMT- E-cadherin and Vimentin
- Metastasis- IL-6 and MMP-2

To evaluate the impact of TLR signaling on the pro-oncogenic effects of HEp-2, we used a commercially available small molecule IRAK-1 &-4 dual inhibitor, which inhibits the kinase activity of IRAK-1 and IRAK-4. We assessed the impact of blocking the TLR signaling on the pro-oncogenic characters by studying the expression of various pro-oncogenic markers associated with survival, proliferative potential, CSCs, metastasis and EMT in HEp-2.

5.3.1 Impact of TLR signaling on the viability of HNSCC cell line

Primarily, we determined the viability of HEp-2 cells count by resazurin-based assay. Treatment with IRAK-1 &-4 dual inhibitor suppressed the number of viable HEp-2 cells in a concentration-dependent manner **(Figure 5.3 A)**. The data suggested that TLR signaling enhances the viable cell proportion.

The dose response curve was plotted using the % viability data **(Figure 5.3 B)**. The IC_{50} and the IC_{25} of IRAK-1 &-4 dual inhibitor on HEp-2, derived from the dose-response curve are listed in **Table 5.1**. The IC_{25} of IRAK-1 &-4 dual inhibitor was selected as a suboptimal dose to treat HEp-2 further in order to evaluate the impact of TLR-IRAK signaling on the pro-oncogenic profile of the cell line.

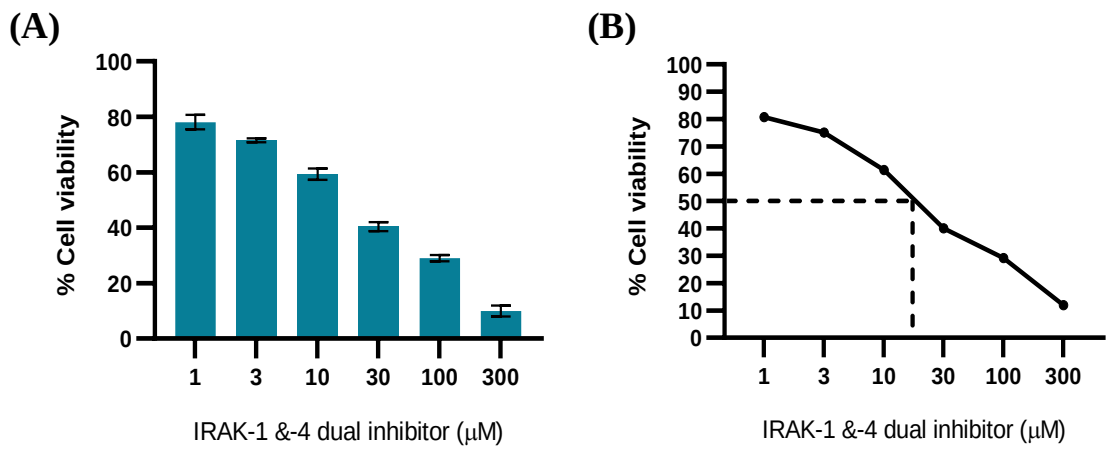

Figure 5.3: Effect of inhibition of the TLR signaling pathway on the viability of HNSCC cell line HEp-2. IRAK-1 &-4 dual inhibitor treatment showing concentration-dependent reduction of HEp-2 cells viability as measured by resazurin assay. Percent cell viability bar graph (A) and curve (B) for IRAK-1 &-4 dual inhibitor treatment from one of the three independent experiments as a representative image is shown.

Table 5.1: IC_{50} and IC_{25} of IRAK-1 &-4 dual inhibitor on HEp-2 cell line

IRAK-1 &-4 dual inhibitor (µM) (n=3)	
IC_{50}	21.58 ± 1.77 µM
IC_{25}	5.1 ± 0.14 µM

5.3.2 Impact of TLR signaling on survival of HNSCC cell line

Bcl-2 and Bcl-xL expression levels were estimated as an indicator of cell survival. The mRNA expression of pro-survival markers *Bcl-2* and *Bcl-xL* were evaluated by qPCR. We found the C_t value of 29.2 ± 0.23 for *Bcl-2* mRNA and C_t value of 31.19 ± 0.75 for *Bcl-xL* mRNA expression in HEp-2. No significant difference in the mRNA fold expression of *Bcl-2* and *Bcl-xL* was observed in HEp-2 after the treatment with IRAK-1 &-4 dual inhibitor **(Figure 5.4)**. This indicated that the TLR signaling did not have any significant impact on the *Bcl-2* and *Bcl-xL* mediated survival of HEp-2 cells.

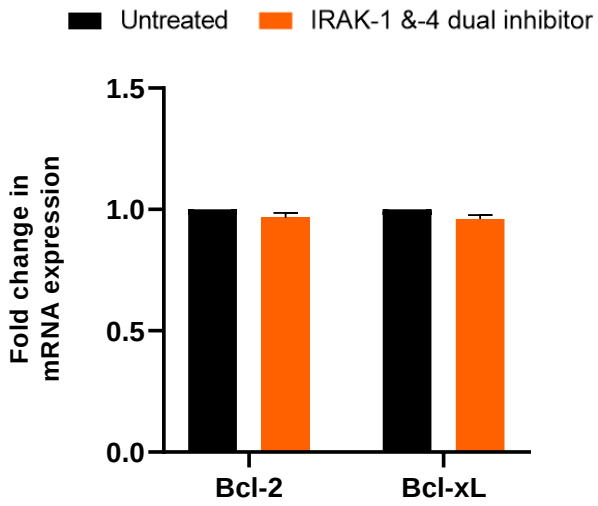

Figure 5.4: Effect of inhibition of the TLR signaling pathway on survival related proteins of HNSCC cell line HEp-2. Bar graph of mRNA fold expression of *Bcl-2* and *Bcl-xL* in HEp-2 with and without IRAK-1 &-4 dual inhibitor as determined by qPCR. Data from three independent experiments is summarized and presented as mean ± S.D.

5.3.3 Impact of TLR signaling on the proliferative potential of HNSCC cell line

To study the impact of TLR signaling on the proliferative potential of HEp-2, the expression of nuclear proliferation antigen Ki-67 was evaluated by intracellular staining using specific antibodies followed by flow cytometry. Approximately 15% of cells in total HEp-2 population were Ki-67+. Treatment with IRAK-1 &-4 dual inhibitor reduced the percentage of Ki-67+ cells by 8%, however the MFI did not alter significantly **(Figure 5.5)**. Data suggested that the TLR signaling had an impact on the proliferative potential of HEp-2.

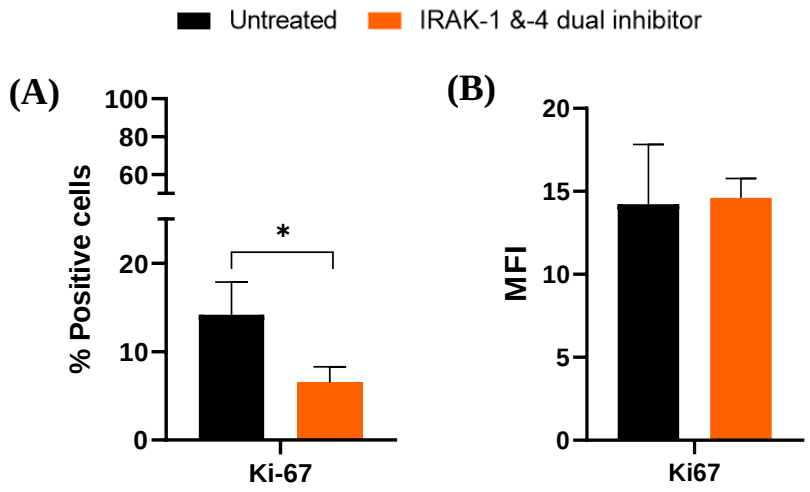

Figure 5.5: Effect of inhibition of the TLR signaling pathway on the proliferative potential of HNSCC cell line HEp-2. (A) Bar graph of Percentage of Ki-67+ HEp-2 cells with and without IRAK-1 &-4 dual inhibitor treatment as determined by flow cytometry. (B) Bar graph of MFI of Ki-67 in HEp-2 with and without IRAK-1 &-4 dual inhibitor treatment determined by flow cytometry. Data from three independent experiments is summarized and presented as mean ± S.D.

5.3.4 Impact of TLR signaling on the CSCs formation in HNSCC cell line

The impact of TLR signaling on CSCs formation was determined by evaluating the expression of CSCs marker CD44, Nanog and ALDH1. The expression of CSCs markers CD44 and Nanog were evaluated by flow cytometry while ALDH1 expression was estimated by western blotting.

Figure 5.6 A shows representative histograms of CD44 expression in HEp-2 after the treatment with IRAK-1 &-4 dual inhibitor. High levels of CD44+ cells (83.2 ± 2.6 %) were detected in HEp-2. IRAK-1 &-4 dual inhibitor treatment did not have any significant effect on the percentage of CD44+ cells or CD44 MFI **(Figure 5.6 B & C-i).**

The level of Nanog+ population of cells was 11.8 ± 2.2 %. No significant effect of IRAK-1 &-4 dual inhibitor treatment was observed on the percentage of Nanog+ cells or Nanog MFI in HEp-2 cells **(Figure 5.6 B & C-ii)**.

High levels of ALDH1 were observed in HEp-2 as evident from its expression level equivalent to GAPDH. Moreover, no alterations in ALDH1 expression in cells were observed upon IRAK-1 &-4 dual inhibitor treatment (1.08-fold) upon densitometric analysis of the bands using the Image J software **(Figure 5.6 D)**. This indicated that the TLR signaling did not have any significant impact on the CSCs of HEp-2.

BST-2 was used as an indirect indicator of stemness. **Figure 5.7 A** shows representative histograms of BST-2 expression in HEp-2 after the treatment with IRAK-1 &-4 dual inhibitor. The level of BST-2+ cells in HEp-2 was 20.91 ± 6.11 %. A significant reduction in percentage of BST-2+ cells in HEp-2 (by 10%) was observed upon IRAK-1 &-4 dual inhibitor treatment **(Figure 5.7 B)**. BST-2 MFI in HEp-2 also reduced significantly upon treatment with IRAK-1 &-4 dual inhibitor **(Figure 5.7 C)**. Further, an association between the expression of BST-2 and CSCs markers was also observed. We found a positive correlation between CD44 MFI and BST-2 MFI ($r=0.8120$, $p=0.0497$) **(Figure 5.7 D)**. We also observed a strong positive correlation between Nanog MFI and BST-2 MFI ($r=0.9393$, $p=0.0054$) **(Figure 5.7 E)**.

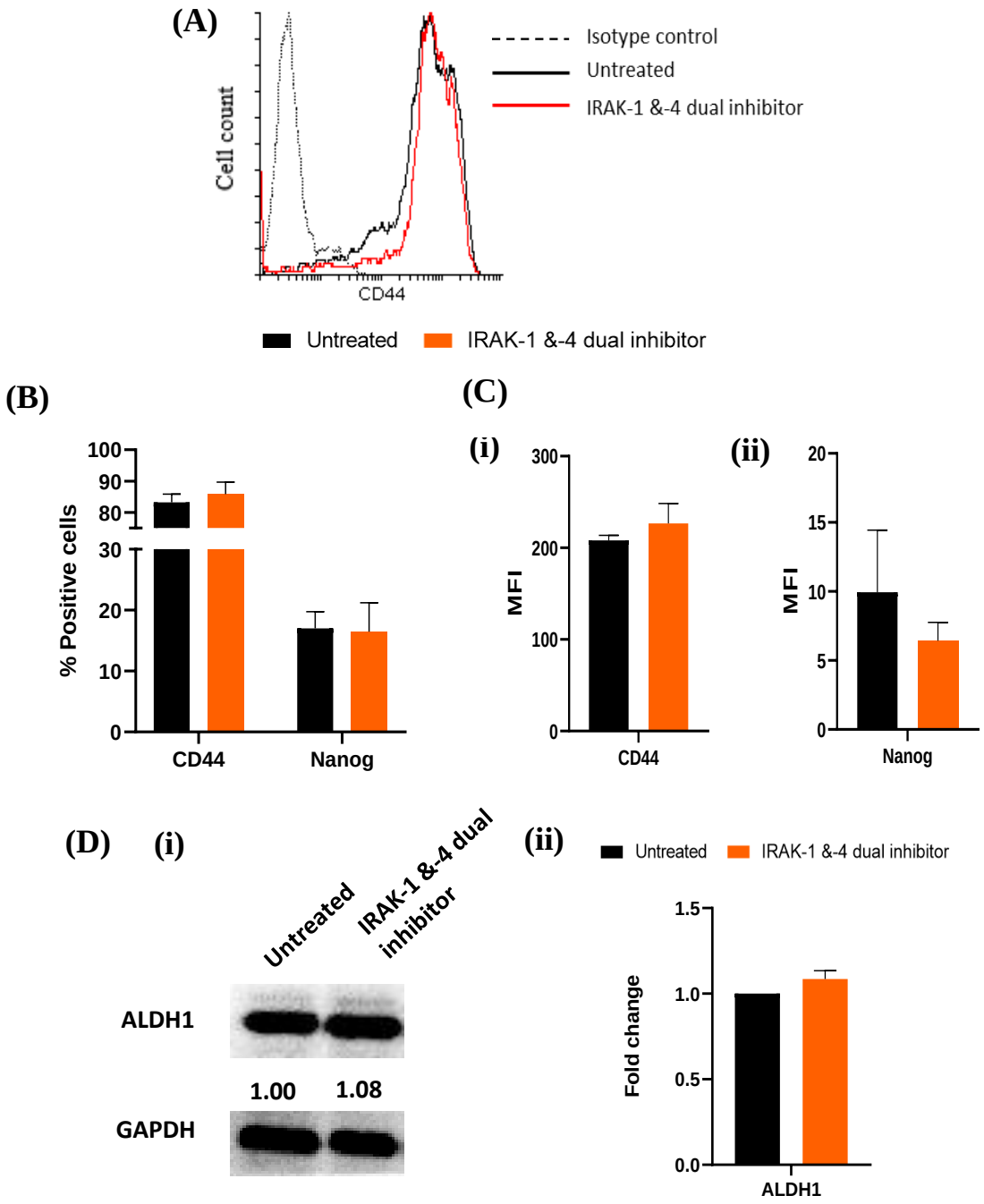

Figure 5.6: Effect of inhibition of the TLR signaling pathway on CSCs using HNSCC cell line HEp-2. (A) Representative histogram image of CD44 expression upon IRAK-1 &-4 dual inhibitor treatment in HEp-2 cells. (B) Bar graph of percentage of CD44+ and Nanog+ HEp-2 cells. (C) Bar graph of MFI of (i) CD44 and (ii) Nanog expressing HEp-2 cells with and without IRAK-1 &-4 dual inhibitor treatment determined by flow cytometry. (D) ALDH1 expression in HEp-2 with and without IRAK-1 &-4 dual inhibitor treatment determined by western blotting. (i) Representative western blot image of one of three independent experiments presented. (ii) Bar graph of relative expression of ALDH1 after normalization with GAPDH and analyzed using Image J software. Data from three independent experiments is summarized and presented as mean ± S.D.

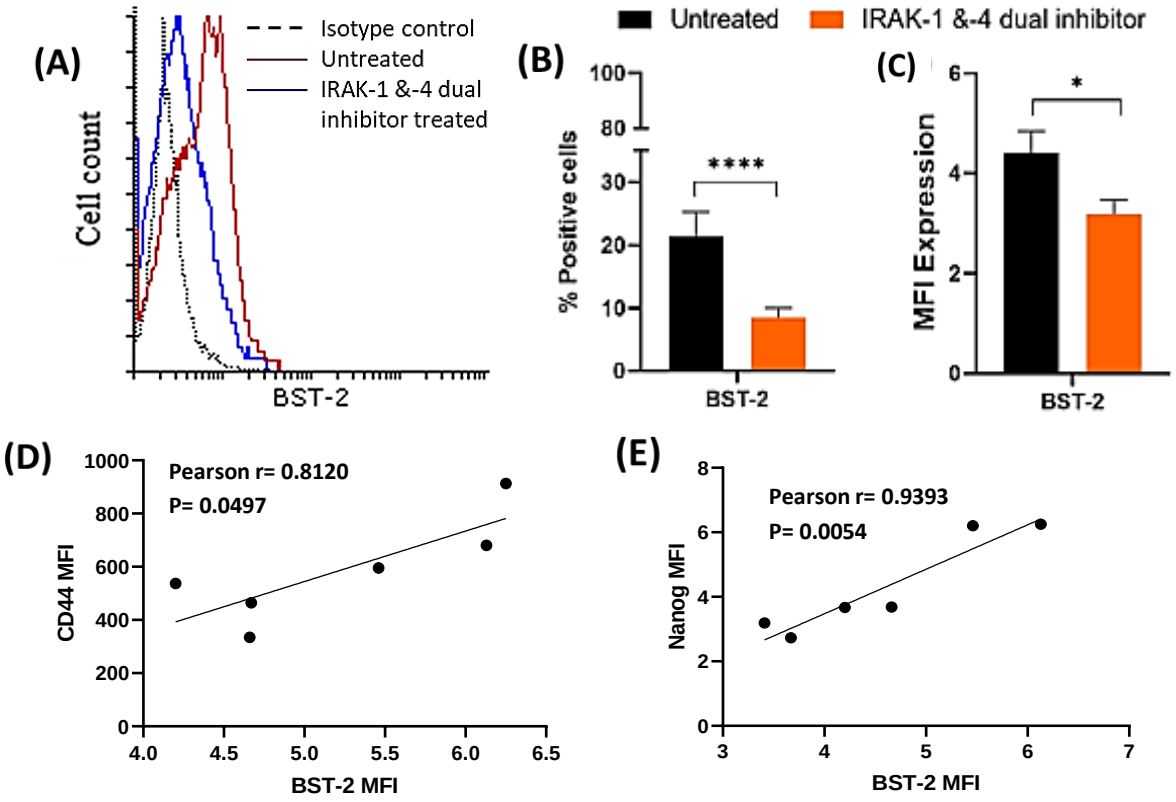

Figure 5.7: Effect of inhibition of the TLR signaling pathway on BST-2 expression and association of BST-2 with CSCs in HNSCC cell line HEp-2 (A) Representative histogram image of BST-2 expression upon IRAK-1 &-4 dual inhibitor treatment in HEp-2. (B) Bar graph of percentage of BST-2+ cells and (C) Bar graph of MFI expression of BST-2 in HEp-2 with and without IRAK-1 &-4 dual inhibitor treatment determined by flow cytometry. (D) Association of BST-2 expression with CD44 expression in HEp-2. (E) Association of BST-2 expression with Nanog expression in HEp-2. Data from more than three independent experiments is summarized and presented as mean ± S.D. (*p<0.05, ****p<0.0001)

5.3.5 Impact of TLR signaling on EMT of HNSCC cell line

To evaluate the impact of TLR signaling on the EMT of HEp-2, the expression of EMT-related proteins E-cadherin and Vimentin were analyzed by flow cytometry. **Figure 5.8 B** shows representative histograms of E-cadherin and Vimentin expression in HEp-2 after the treatment with IRAK-1 &-4 dual inhibitor. A large proportion of HEp-2 cells expressed E-cadherin (87 ± 2.8 %) although proportion of Vimentin+ cells were only 14.8 ± 1.2 % **(Figure 5.8 A & C)**. IRAK-1 &-4 dual inhibitor treatment neither altered the percentage nor MFI of E-cadherin and Vimentin expressing cells **(Figure 5.8 C & D)**. This data suggested that the TLR signaling do not contribute to the EMT of HEp-2.

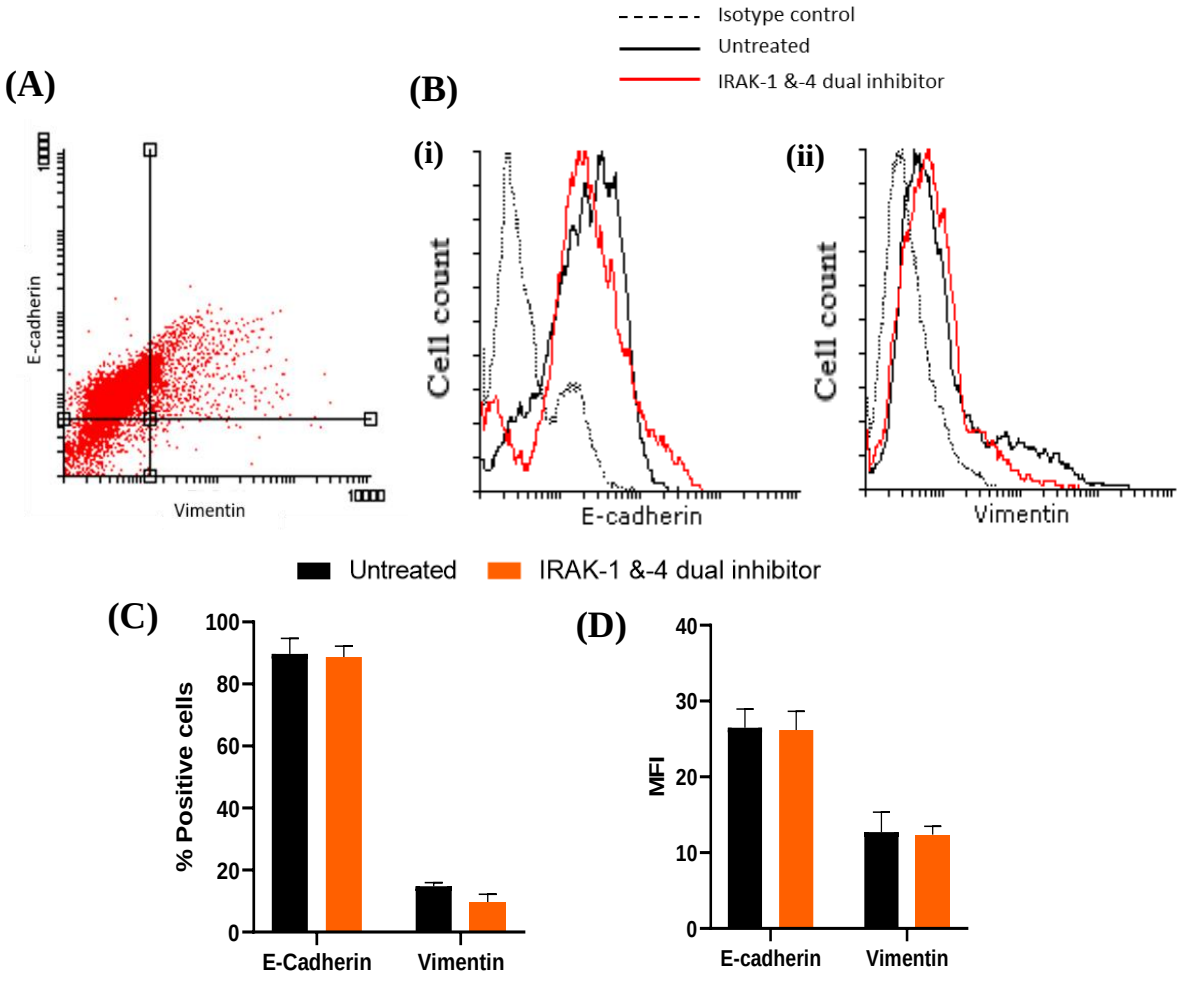

Figure 5.8: Effect of inhibition of the TLR signaling pathway on the EMT of HNSCC cell line HEp-2. (A) Dot plot demonstrating expression of E-cadherin and Vimentin on HEp-2. (B) Representative histogram images of (i) E-cadherin and (ii) Vimentin expression on HEp-2 cells with and without IRAK-1 &-4 dual inhibitor treatment. Bar graphs of (C) percentage and (D) MFI expression of E-cadherin+ and Vimentin+ HEp-2 cells with and without IRAK-1 &-4 dual inhibitor treatment determined by flow cytometry. Data from three independent experiments is summarized and presented as mean ± S.D.

5.3.6 Impact of TLR signaling on the metastasis of HNSCC cell line

MMP-2 and IL-6 are shown to be associated with metastasis in oral cancer cells. Both are eshtablished diagnostic markers of metastasis. The impact of TLR signaling on the metastasis of HEp-2 was determined by evaluating the expression of MMP-2 and IL-6. The mRNA expression of *MMP-2* was observed on HEp-2 (C_t=27.21 ± 0.23) which remained unchanged upon treatment with IRAK-1 &-4 dual inhibitor (C_t=26.94 ± 0.92) **(Figure 5.9 A).**

IL-6 levels were determined by ELISA. 2033 ± 133 pg/mL of IL-6 cytokine were detected in the supernatant of HEp-2 cells. Treatment with IRAK-1 &-4 dual inhibitor showed no significant effect on the these levels (2259 ± 684 pg/mL) **(Figure 5.9 B)**. These results suggested that the TLR signaling do not contribute to the metastasis of HEp-2 cells.

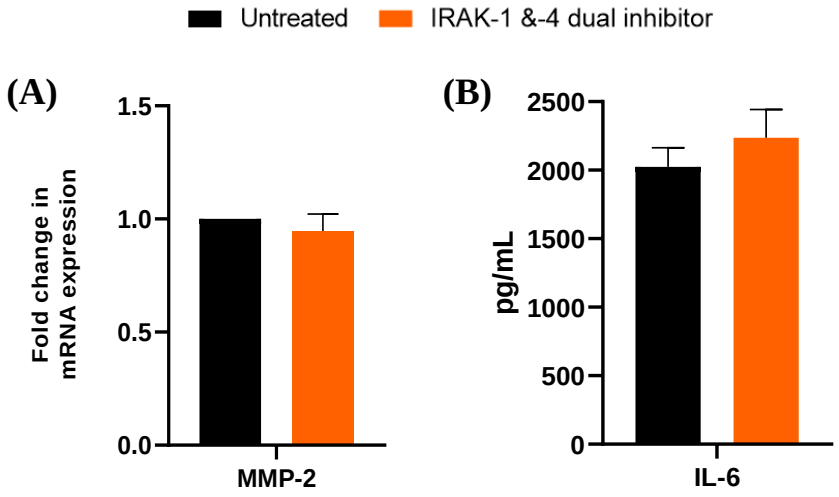

Figure 5.9: Effect of inhibition of the TLR signaling pathway on the metastasis of HNSCC cell line HEp-2. (A) Bar graph of mRNA fold expression of *MMP-2* in HEp-2 with and without the treatment with IRAK-1 &-4 dual inhibitor determined by qPCR. (B) Bar graph of IL-6 secretion by HEp-2 cells with and without the treatment with IRAK-1 &-4 dual inhibitor evaluated by ELISA. Data from three independent experiments is summarized and presented as mean ± S.D.

5.4 Evaluation of the role of TLR signaling in chemo-resistant HNSCC

We developed an *in-vitro* cell line-based model to mimic chemo-resistance to TPF treatment using HEp-2. Using this model, we evaluated the role of TLR signaling on the oncogenic properties of the chemo-resistant HNSCC.

5.4.1 Determination of IC_{50} of chemo-drugs on HNSCC cell line

The IC_{50} of the chemo-drugs—docetaxel, cisplatin and 5-FU— on HEp-2 were determined by resazurin assay. **Figure 5.10** demonstrates the dose-response curves from which the $IC_{50,}$ $IC_{6.25}$ and $IC_{3.125}$ for each chemo-drug were derived that were utilized for the development of a triple-chemo-resistant cell line as described in ***Materials and methods, 4.2.1.2 Development of triple chemo-resistant cell line.*** The $IC_{50,}$ $IC_{6.25}$ and $IC_{3.125}$ of the chemo-drugs observed on HEp-2 cells are presented in **Table 5.2**.

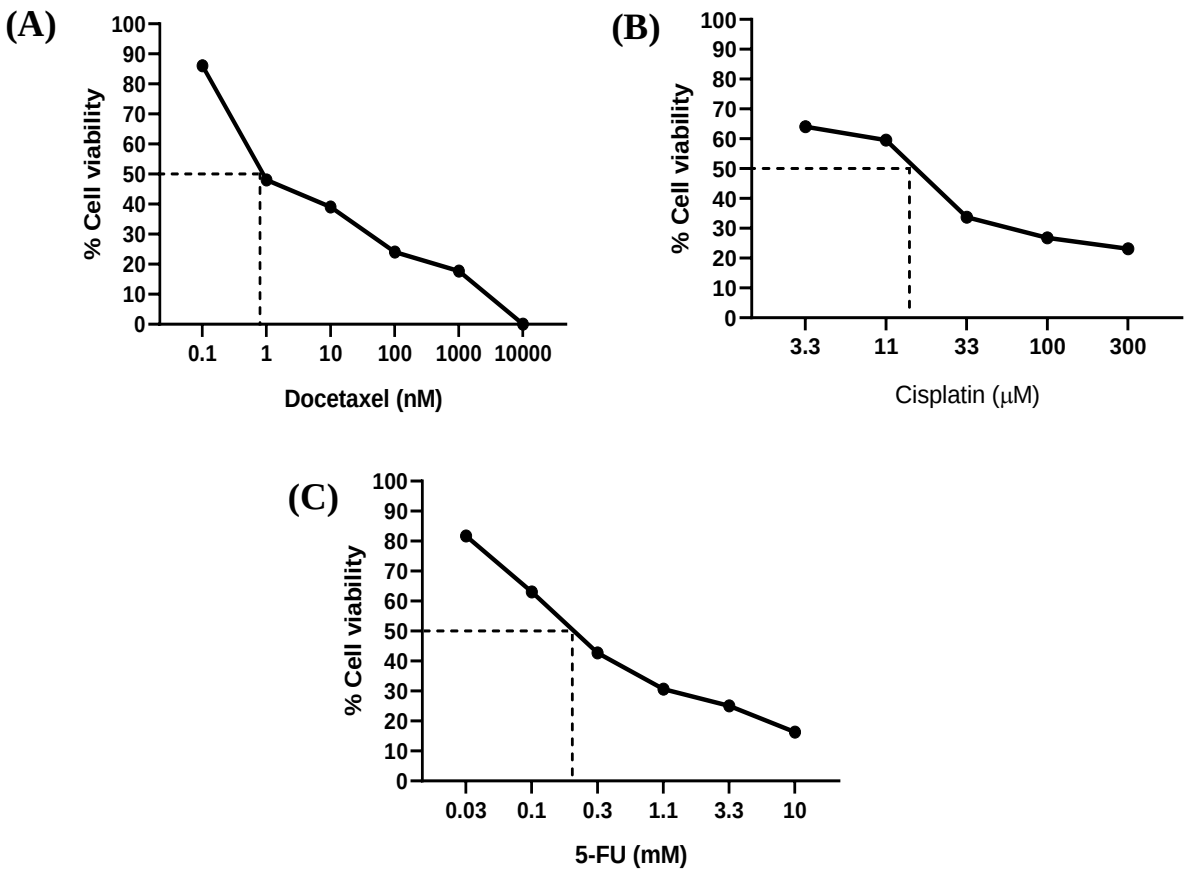

Figure 5.10: Effect of chemo-drug treatment on the viability of HEp-2 cell line. Treatment with Docetaxel (A), Cisplatin (B) and 5-FU (C) showing concentration-dependent inhibition in viability of HEp-2 as measured by resazurin assay. Percent cell viability curve for each chemo-drug treatment on cells from one of the six independent experiments as a representative image is shown.

Table 5.2: IC_{50}, $IC_{6.25}$ and $IC_{3.125}$ values of the chemo-drugs on HEp-2 cell line

	Docetaxel (nM) (n=6)	Cisplatin(µM) (n=6)	5-FU (mM) (n=6)
IC_{50}	0.864 ± 0.42	13.05 ± 3.31	0.237 ± 0.06
$IC_{6.25}$	0.056 ± 0.04	0.826 ± 0.18	0.010 ± 0.01
$IC_{3.125}$	0.030 ± 0.02	0.665 ± 0.16	0.004 ± 0.01

5.4.2 Morphological characteristics of the triple-chemo-resistant HNSCC cell line

Assessment of the differences in the morphological features were observed with an enlarged cell size and nuclei of the chemo-resistant cells as compared to the parent cells **(Figure 5.11 A)**. Using similar voltage settings, the FSC vs SSC profile of both the cell lines were evaluated by flow cytometry. Comparatively higher SSC signals for chemo-resistant HEp-2 than the Parent HEp-2 as observed indicated increase in the granularity of the chemo-resistant cell line **(Figure 5.11 B)**. Comparatively higher FSC signals were observed demonstrating increased cell size of the chemo-resistant cells than parent cells **(Figure 5.11 C)**.

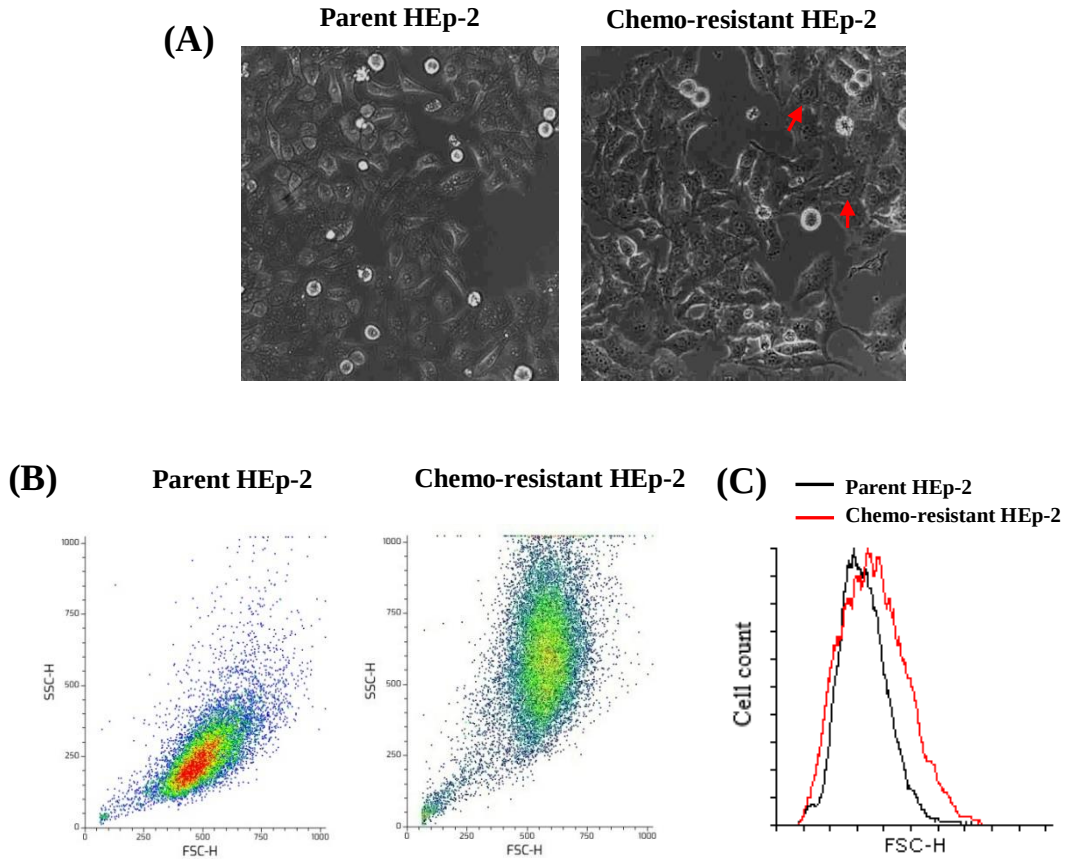

Figure 5.11: Assessment of morphological features of chemo-resistant cell line. (A) Representative phase-contrast micrograph images demonstrating enlarged cell size and nuclei (indicated by arrows) in the chemo-resistant HEp-2 as compared to parent cell line. Images presented at original magnification, 40X. (B) Representative FSC vs. SSC scatter plots of parent and chemo-resistant cells analyzed by flow cytometry (C) Representative FSC histogram image of parent and chemo-resistant HEp-2 cells.

5.4.3 Validation of the acquired chemo-resistance of the triple-chemo-resistant HNSCC cell line

A triple-chemo-resistant cell line was developed by exposing HEp-2 cells to a combination of the three chemo-drugs in a sequential manner. To validate the chemo-resistance development, the IC_{50} of the chemo-drugs on the resistant cells were evaluated using same method and compared to the IC_{50} of the chemo-drugs on the parent cells **(Figure 5.12 and Table 5.3)**. A fold increase of 1686, 4 and 12 in the IC_{50} of Docetaxel, Cisplatin and 5-FU, respectively was observed on the chemo-resistant cells compared to parent cells. These results validated the acquisition of resistance in the claimed chemo-resistant cell line.

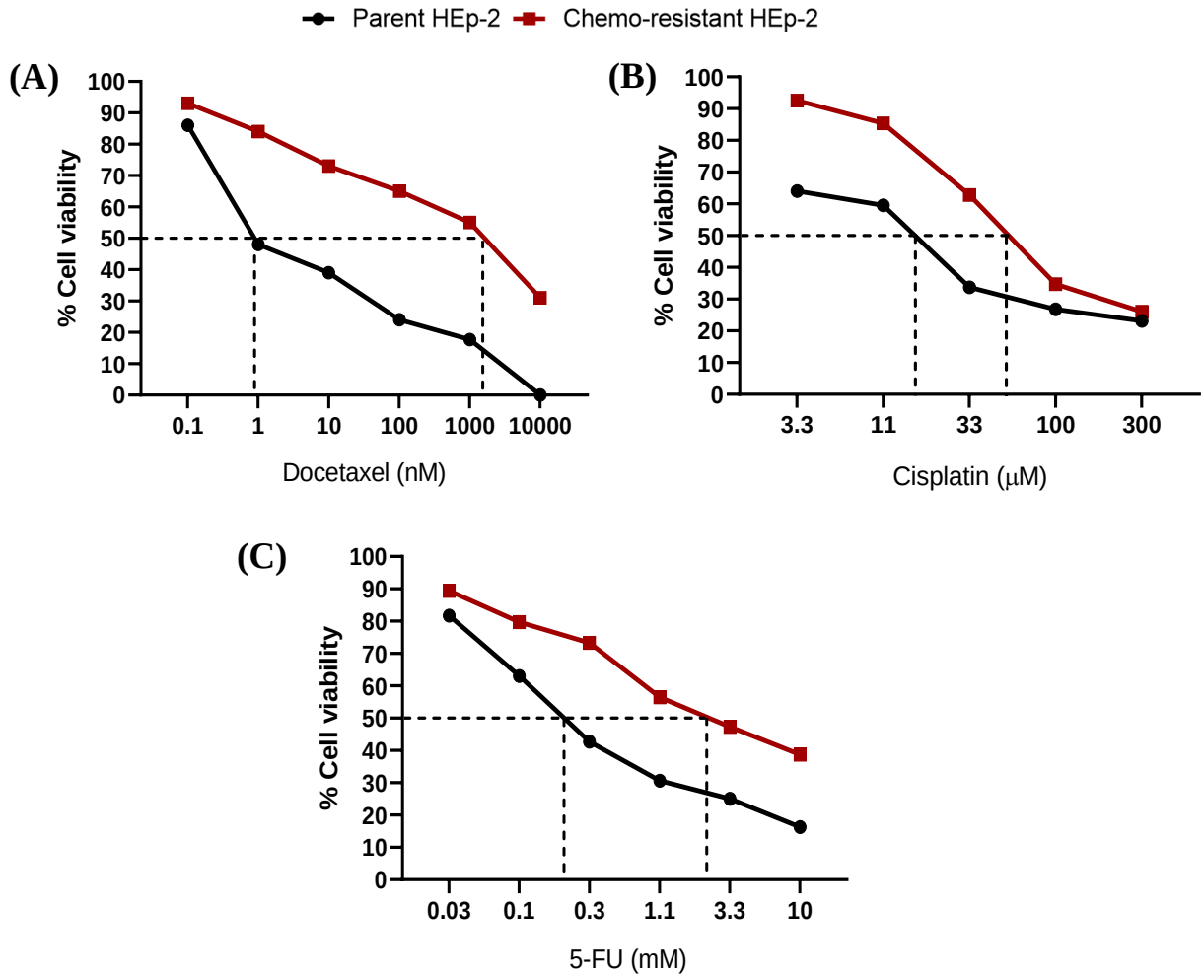

Figure 5.12: Validation of the acquired chemo-resistance of the developed triple-chemo-resistant cell line. Cell viability-based dose response curve for chemo-drugs Docetaxel (A), Cisplatin (B) and 5-FU (C) on chemo-resistant and parent HEp-2 determined by resazurin assay. Percent cell viability curve for each treatment on cells from one of six independent experiments as a representative image is shown.

Table 5.3: Comparison of the IC_{50} values of chemo-drugs on parent and chemo-resistant HEp-2

Chemo drug	Parent HEp-2 (n=6)	Chemo-resistant HEp-2 (n=6)	Fold change (Increase in IC_{50} value on chemo-resistant HEp-2 wrt Parent HEp-2)
Docetaxel	0.864 ± 0.42 nM	1450 ± 0.7 nM	1686
Cisplatin	13.05 ± 3.31 µM	53.04 ± 4.88 µM	4
5-FU	0.237 ± 0.062 mM	2.8 ± 0.8 mM	12

5.4.4 Evaluation of TLRs 1-10 expression on chemo-resistant HNSCC cell line

Further, to evaluate the TLR expression profile in chemo-resistant HEp-2, we quantitated the mRNA expression of TLRs 1-10 by qPCR. The average C_t values of TLRs observed on the resistant line are presented in **Figure 5.13**. Using $\Delta\Delta C_t$ calculations, all the other TLRs showed equivalent level of mRNA expression between the parent and chemo-resistant HEp-2 with absence of TLR 2 and TLR 10 (C_t above 35) **(Figure 5.14)**.

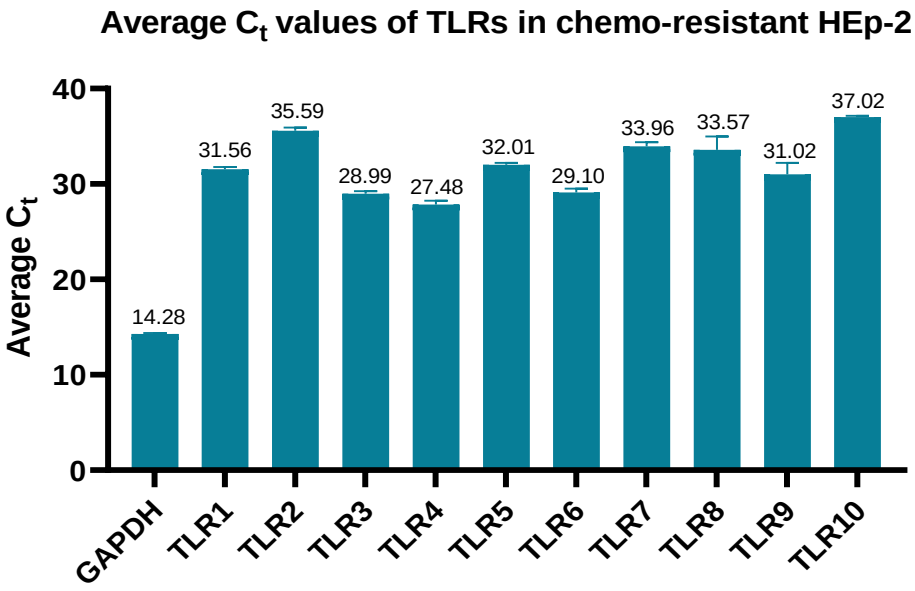

Figure 5.13: Expression of TLRs in chemo-resistant HEp-2 cell line. Bar graph of average C_t values of TLRs in chemo-resistant HEp-2 determined by qPCR.

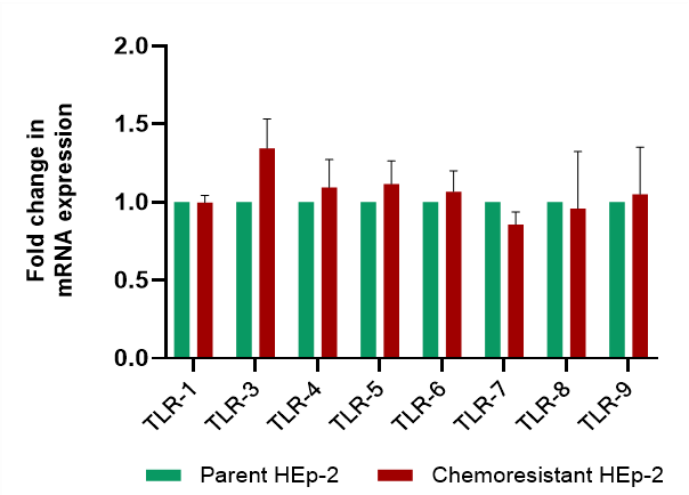

Figure 5.14: Comparative analysis of mRNA expression of TLRs 1-10 on parent and chemo-resistant HEp-2 cell line. Bar graph of fold change in mRNA expression of TLRs 1-10 on chemo-resistant HEp-2 compared with parent HEp-2. Data from three independent experiments is summarized and presented as mean ± S.D. (****p<0.0001)

5.4.5 Evaluation of constitutive TLR signaling in chemo-resistant HNSCC cell line

To examine whether the constitutive TLR signaling is active in chemo-resistant HEp-2, expression and phosphorylation of downstream molecules involved in TLR signaling namely IRAK-1 and IRAK-4, were evaluated by flow cytometry.

Figure 5.15 A shows representative histograms comparing expression of IRAK-1, IRAK-4 and their phosphorylated forms in parent and chemo-resistant cells. 31.71±2.01% of total chemo-resistant HEp-2 cells were IRAK-1+ of which 25.66 ± 2.3% were phosphorylated. This data indicated that 80.75% of IRAK-1+ cells in chemo-resistant HEp-2 were existing in their activated state. Compared with parent HEp-2, these levels were 2.8-fold and 5.6-fold more for IRAK-1+ and p-IRAK-1+ cells, respectively in chemo-resistant HEp-2 **(Figure 5.15 B)**.

27.5 ± 0.51% of total chemo-resistant HEp-2 cells were IRAK-4+ of which 25.49 ±1.54% were phosphorylated. This data indicated that 92.6% of IRAK-4+ cells in chemo-resistant HEp-2 were existing in their activated state. Compared with parent HEp-2, these levels were 2.5-fold and 2.87-fold more for IRAK-4+ and p-IRAK-4+ cells, respectively in chemo-resistant HEp-2 **(Figure 5.15 B)**.

Apart from this, a significant increase in the MFI expression of IRAK-1, IRAK-4 and their phosphorylated forms in the chemo-resistant HEp-2 compared to parent HEp-2 was also observed **(Figure 5.15 C)**. Results suggested an activated IRAK mediated TLR signaling in chemo-resistant HEp-2 with a comparatively higher intensity than the signaling in parent HEp-2.

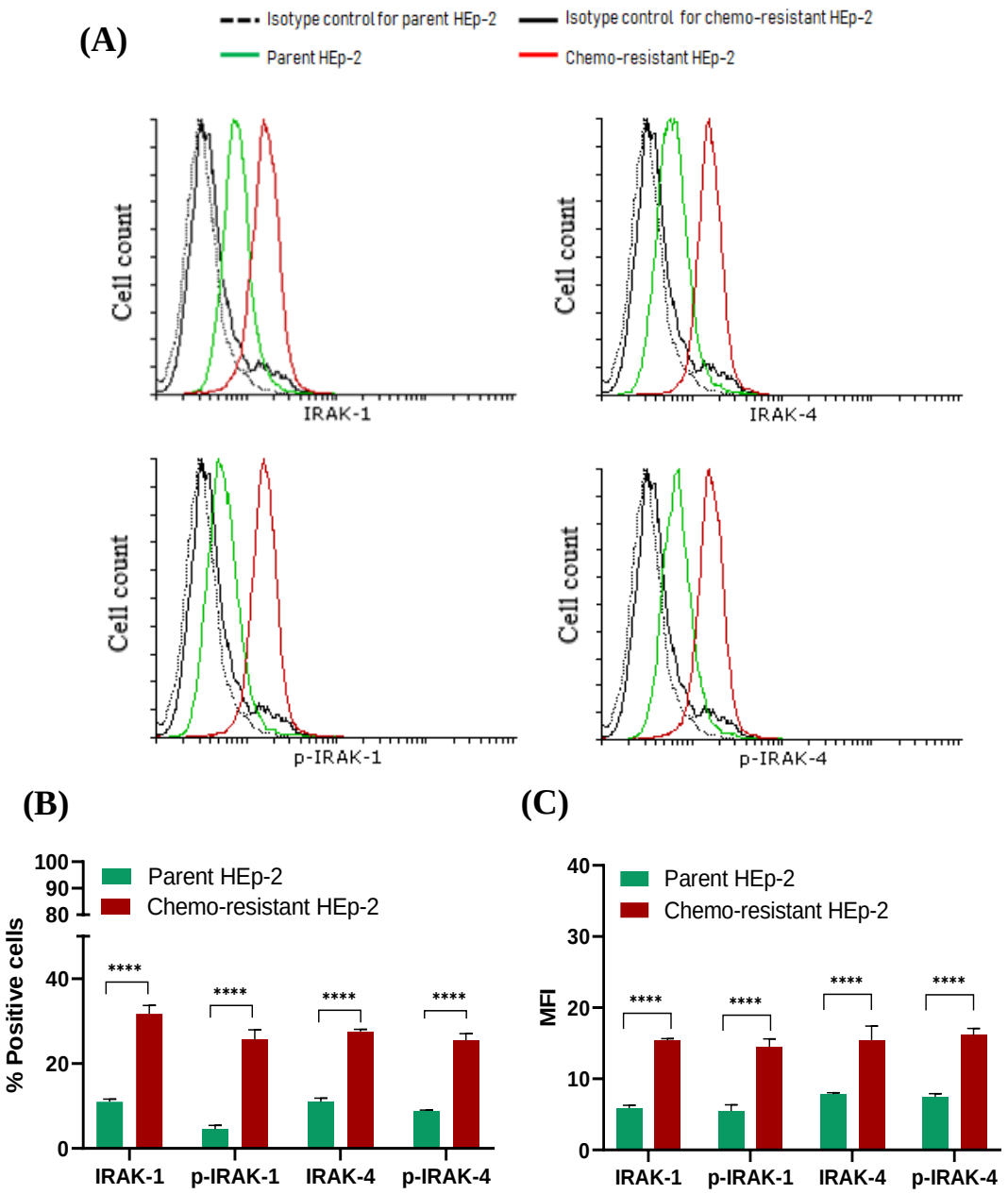

Figure 5.15: IRAK-signaling in chemo-resistant HEp-2 cell line. (A) Representative flow cytometric histogram images for IRAK-1, p-IRAK-1, IRAK-4 and p-IRAK-4 expression. (B) Bar graph of percentage of IRAK-1+, p-IRAK-1+, IRAK-4+ and p-IRAK-4+ cells in chemo-resistant HEp-2 compared to parent HEp-2 determined by flow cytometry. (C) Bar graph of IRAK-1, p-IRAK-1, IRAK-4 and p-IRAK-4 MFI in chemo-resistant HEp-2 compared to parent HEp-2 determined by flow cytometry. Data from three independent experiments is summarized and presented as mean ± S.D. (****p<0.0001.)

5.4.6 Impact of inhibition of TLR signaling pathway on viability of chemo-resistant HNSCC cell line

Viability of the chemo-resistant cells was evaluated upon inhibition of the TLR signaling in cells. Treatment with IRAK-1 &-4 dual inhibitor suppressed the viability of the chemo-resistant cells in a concentration-dependent manner **(Figure 5.16)**. A 5-fold increase in the IC_{50} of IRAK-1 &-4 dual inhibitor on the chemo-resistant cells compared to parent cells was observed **(Table 5.4)**. The IC_{25} of IRAK-1 &-4 dual inhibitor observed on the chemo-resistant cell line was 15.2 ± 0.351 µM.

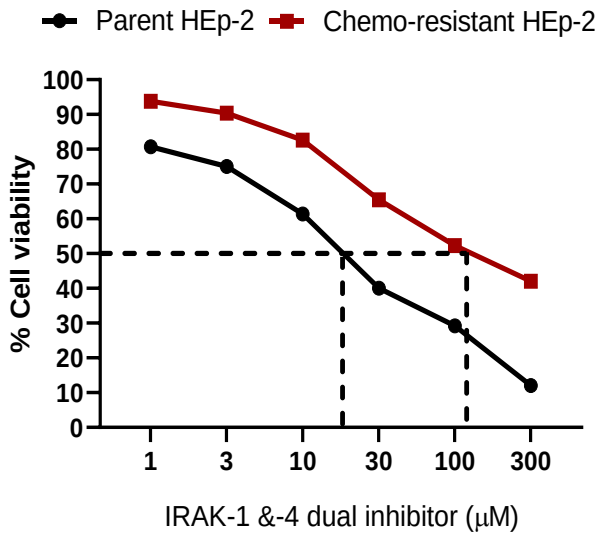

Figure 5.16: Effect of IRAK-1 &-4 dual inhibitor treatment on the viability of chemo-resistant HEp-2 cell line. IRAK-1 &-4 dual inhibitor treatment demonstrating concentration-dependent inhibition of cell viability of chemo-resistant HEp-2 assessed by resazurin assay. Percentage cell viability curves comparing the effect of IRAK-1 &-4 dual inhibitor on parent and chemo-resistant HEp-2 shown as a representative image from one of the three independent experiment.

Table 5.4.: Comparison of IC_{50} values of IRAK-1 &-4 dual inhibitor on parent and chemo-resistant HEp-2

	Parent HEp-2 (n=3)	**Chemo-resistant HEp-2 (n=3)**	**Fold Change (Increase in IC_{50} value on chemo-resistant HEp-2 wrt Parent HEp-2 cell line)**
IC_{50} of IRAK-1 &-4 dual inhibitor	21.58 ± 1.77 µM	121.31 ± 22.53 µM	5

5.4.7 Impact of TLR signaling on the pro-oncogenic properties of chemo-resistant HNSCC cell line

To evaluate the dependence of the pro-oncogenic features of the chemo-resistant cell line on the TLR signaling pathway, we characterized the expression of the survival, proliferation, CSCs formation, metastasis and EMT markers in the chemo-resistant cell line with and without inhibition of the TLR signaling pathway using IRAK-1 &-4 dual inhibitor.

5.4.7.1 Impact of TLR signaling on the survival of chemo-resistant HNSCC cell line

A 6.3-fold over-expression in *Bcl-2* mRNA and a 4.4-fold over-expression in the mRNA of *Bcl-xL* in the resistant cell line compared to the parent cell line was observed. Treatment with IRAK-1 &-4 dual inhibitor suppressed the mRNA expression of *Bcl-2* in the chemo-resistant cell line by 5.5-fold whereas the mRNA expression of *Bcl-xL* was undetectable. The C_t values are presented in **Table 5.5**. Of the two cell lines, IRAK-1 &-4 dual inhibitor treatment was distinctly effective in suppressing the mRNA expression of survival markers in the chemo-resistant cells. The levels of *Bcl-2* mRNA in IRAK-1 &-4 dual inhibitor treated chemo-resistant HEp-2 were low than those compared to parent HEp-2. *Bcl-xL* mRNA levels in IRAK-1 &-4 dual inhibitor treated chemo-resistant HEp-2 were drastically reduced in comparison to those of parent HEp-2 **(Figure 5.17)**.

Table 5.5: C_t values of *Bcl-2* and *Bcl-xL* mRNA in the chemo-resistant cell line with and without IRAK-1 &-4 dual inhibitor treatment

	C_t values on chemo-resistant cell line	
Gene	**Untreated**	**IRAK-1 &-4 dual inhibitor treated**
Bcl-2	26.23 ± 0.37	29.97 ± 0.37
Bcl-xL	29.13 ± 0.70	37.33 ± 0.72

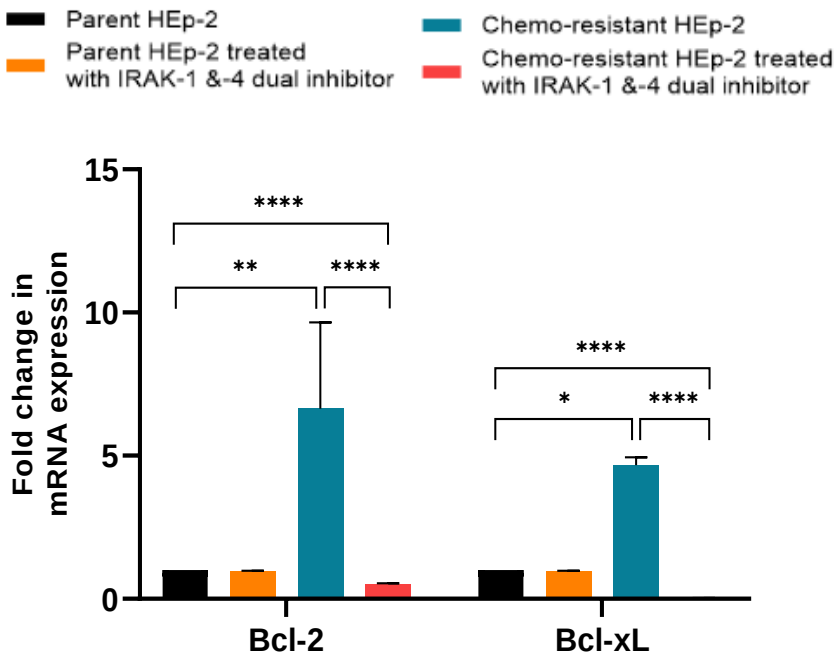

Figure 5.17: Effect of inhibition of the TLR signaling pathway on the expression of survival related proteins of chemo-resistant HEp-2 cell line. Bar graph of mRNA fold expression of *Bcl-2* and *Bcl-xL* in chemo-resistant HEp-2 compared to parent HEp-2 with and without treatment of IRAK-1 &-4 dual inhibitor. Data from three independent experiments is summarized and presented as mean ± S.D. (*p<0.05, **p<0.01, ****p<0.0001)

5.4.7.2 Impact of TLR signaling on the proliferative potential of chemo-resistant HNSCC cell line

The proliferative potential of the chemo-resistant cell line was assessed by evaluating the expression of Ki-67 by flow cytometry. **Figure 5.18 A** shows representative histograms of Ki-67 expression in parent and chemo-resistant HEp-2. We observed 22 ± 5.5% Ki-67+ cells in the chemo-resistant cell line which was a 3-fold increase compared to the parent cell line (7.4 ± 1.2 %) **(Figure 5.18 C)**. A significant decrease in the percentage of Ki-67+ cells, but not in Ki-67 MFI of the chemo-resistant cells was observed upon treatment with IRAK-1 &-4 dual inhibitor **(Figure 5.18 C & D)** and the data is represented as histograms in **Figure 5.18 B**. Of the two cell lines, IRAK-1 &-4 dual inhibitor treatment was effective in downregulating the expression of Ki-67 in the chemo-resistant cell line. After the treatment of chemo-resistant cell line with IRAK-1 &-4 dual inhibitor, the levels of Ki-67+ cells were decreased significantly with the levels becoming equivalent to levels of Ki-67+ parent cells.

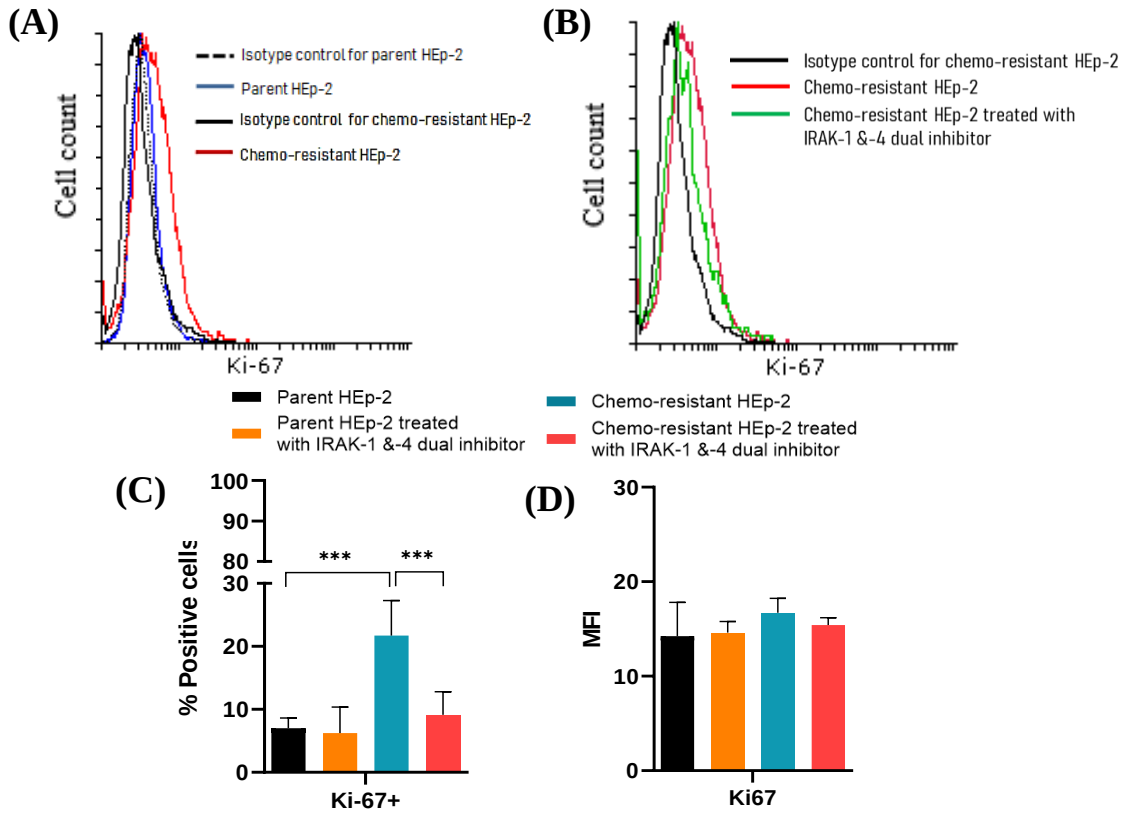

Figure 5.18: Effect of inhibition of the TLR signaling pathway on the proliferative potential of chemo-resistant HEp-2 cell line. (A) Representative flow cytometry histograms demonstrating Ki-67 expression in parent and chemo-resistant HEp-2 (B) Representative flow cytometry histograms demonstrating Ki-67 expression in chemo-resistant HEp-2 treated with IRAK-1 &-4 dual inhibitor. Bar graph of (C) percentage of Ki-67+ cells and (D) Ki-67 MFI in chemo-resistant and parent HEp-2 with and without IRAK-1 &-4 dual inhibitor treatment determined by flow cytometry. Data from three independent experiments is summarized and presented as mean ± S.D. (***p<0.001)

5.4.7.3 Impact of TLR signaling on the CSCs formation of chemo-resistant HNSCC cell line

Assessment of expression of CSCs through markers CD44 and Nanog in the chemo-resistant HEp-2 was performed by flow cytometry. **Figure 5.19 A & B** shows representative histograms of CD44 and Nanog expression in parent and chemo-resistant HEp-2.

98.3 ± 1.13 % CD44+ cells were observed in chemo-resistant HEp-2 which was marginally more (1.2-fold) than that observed in parent HEp-2 (83.2 ± 2.6 %) **(Figure 5.19 D)**. A significant increase in CD44 MFI in chemo-resistant HEp-2 compared to parent HEp-2 was observed. Treatment with IRAK-1 &-4 dual inhibitor did not have any significant effect in the suppression of CD44+ cells or CD44 MFI in HEp-2 and the levels of CD44 in parent and chemo-resistant HEp-2 post treatment remain unchanged **(Figure 5.19 E)**.

18.45 ± 2.02 % Nanog+ cells were observed in chemo-resistant HEp-2 which were 1.5-fold more as observed in parent HEp-2 (11.8 ± 2.5 %). A significant decrease in the percentage of Nanog+ chemo-resistant cells (10 ± 1.2%) was observed upon treatment with IRAK-1 &-4 dual inhibitor **(Figure 5.19 D)** and the data is represented as histogram in **Figure 5.19 C**. These suppressed levels were equivalent to the levels of Nanog+ cells observed in parent HEp-2 treated with IRAK-1 &-4 dual inhibitor. There were no significant alterations in Nanog MFI before and after IRAK-1 &-4 dual inhibitor treatment in either chemo-resistant HEp-2 or parent HEp-2 **(Figure 5.19 F)**.

Marginal over-expression (1.1-fold) of ALDH1 was detected in chemo-resistant HEp-2 compared to parent HEp-2 as determined by western blotting. A minimal reduction in ALDH1 expression (by 0.3-fold) in the chemo-resistant cells upon treatment with IRAK-1 &-4 dual inhibitor was observed. The levels of ALDH1 post treatment with IRAK-1 &-4 dual inhibitor in chemo-resistant and parent cell line were found equal **(Figure 5.20 A & B)**.

Figure 5.21 A shows representative histograms of BST-2 expression in parent and chemo-resistant HEp-2. By flow cytometric analysis, 82 ± 3.5 % BST-2+ cells were observed in chemo-resistant HEp-2 which were 4-fold more compared to BST-2+ cells in parent HEp-2 (20.91 ± 6.11 %). BST-2 MFI was observed as 292 ± 2.5 in chemo-resistant HEp-2 which was 48-fold more than BST-2 MFI in parent HEp-2 (6 ± 1.7). Treatment with IRAK-1 &-4 dual inhibitor did not alter the levels of BST-2 in the chemo-resistant cells **(Figure 5.21 B & C)**.

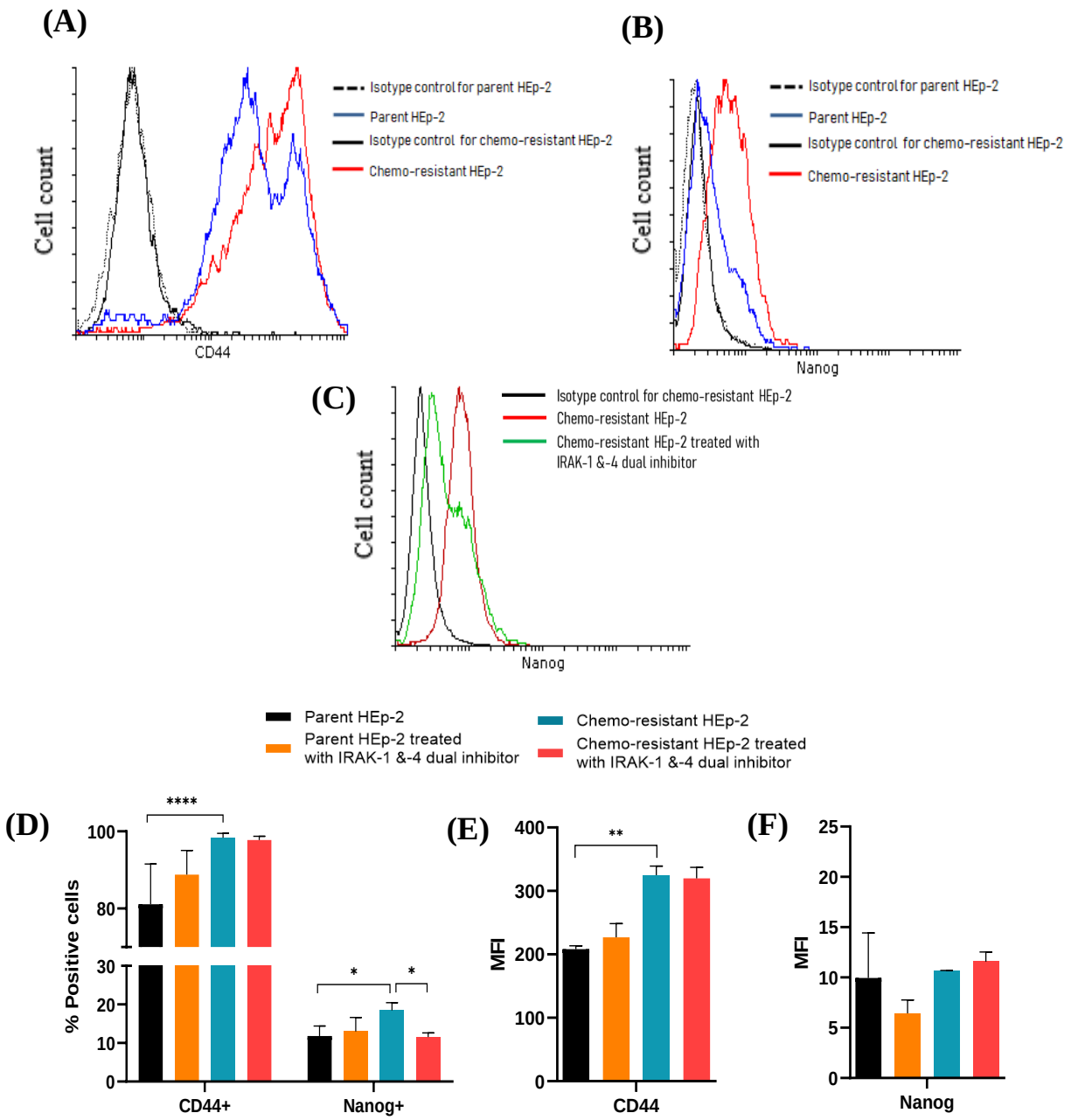

Figure 5.19: Effect of inhibition of the TLR signaling pathway on the CD44 and Nanog expression of chemo-resistant HEp-2 cell line. (A) Representative flow cytometric histogram image for CD44 expression in parent and chemo-resistant HEp-2 cells (B) Representative flow cytometric histogram image for Nanog expression in parent and chemo-resistant HEp-2 cells. (C) Representative flow cytometric histogram image for Nanog expression in IRAK-1 &-4 dual inhibitor treated chemo-resistant HEp-2 cells. (D) Bar graph of percentage of CD44+ and Nanog+ cells in chemo-resistant and parent HEp-2 with and without IRAK-1 &-4 dual inhibitor treatment determined by flow cytometry. (E) Bar graph of CD44 MFI in chemo-resistant and parent HEp-2 with and without IRAK-1 &-4 dual inhibitor treatment determined by flow cytometry. (F) Bar graph of Nanog MFI in chemo-resistant and parent HEp-2 with and without IRAK-1 &-4 dual inhibitor treatment determined by flow cytometry. Data from three independent experiments is summarized and presented as mean ± S.D. (*p<0.05, **p<0.01, ****p<0.0001).

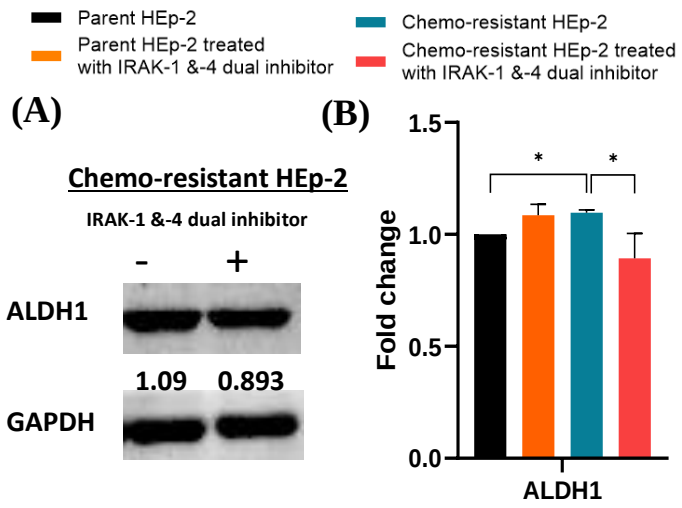

Figure 5.20: Effect of inhibition of the TLR signaling pathway on the ALDH1 expression in chemo-resistant HEp-2 line. Western blotting analysis of ALDH1 expression in chemo-resistant HEp-2 compared to parent HEp-2 with and without IRAK-1 &-4 dual inhibitor treatment. (A) Representative western blot image of one of three independent experiments presented. (B) Bar graph of relative expression of ALDH1 after normalization with GAPDH analyzed by Image J software (NIH, USA). Data from three independent experiments is summarized and presented as mean ± S.D. (*p<0.05).

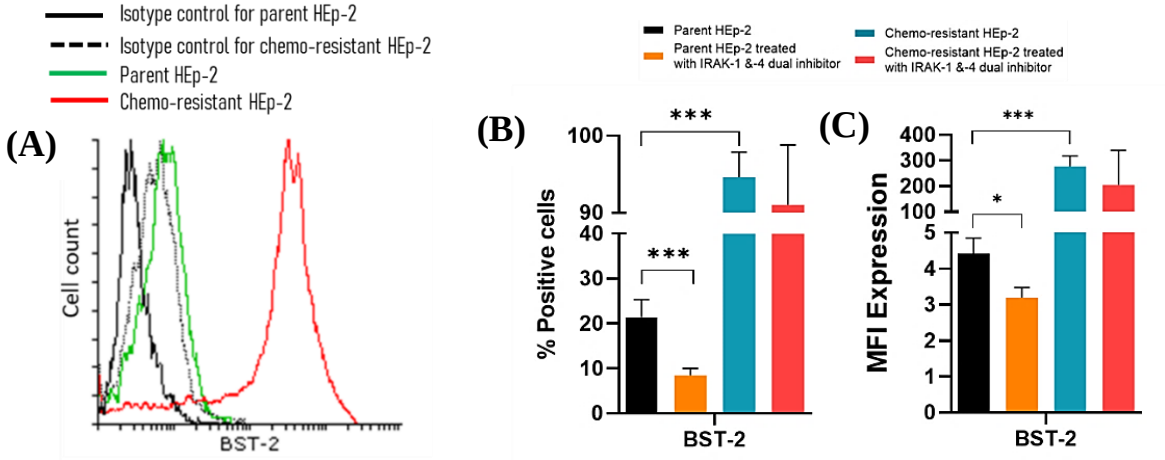

Figure 5.21: Effect of inhibition of the TLR signaling pathway on the BST-2 expression of chemo-resistant HEp-2 cell line. (A) Representative flow cytometric histogram image for BST-2 expression in parent and chemo-resistant HEp-2 cells. (B) Bar graph of percentage of BST-2+ expressing chemo-resistant and parent HEp-2 cells with and without IRAK-1 &-4 dual inhibitor treatment determined by flow cytometry. (C) Bar graph of BST-2 MFI in chemo-resistant and parent HEp-2 cells with and without IRAK-1 &-4 dual inhibitor treatment determined by flow cytometry. Data from three independent experiments is summarized and presented as mean ± S.D. (*p<0.05, ***p<0.001).

5.4.7.4 Impact of TLR signaling on the EMT of chemo-resistant HNSCC cell line

Flow cytometric analysis demonstrated 39.5 ± 5.9 % E-cadherin+ cells in the chemo-resistant cell line which were 2-fold reduced in comparison to the levels of E-cadherin+ cells in parent cell line (89.6 ± 4.03 %) **(Figure 5.22 D)**. The data is represented as histograms in **Figure 5.22 A**. IRAK-1 &-4 dual inhibitor treatment further reduced the E-cadherin+ cells in chemo-resistant cell line by 20 ± 2.2% **(Figure 5.22 D)**. No significant alterations were observed in E-cadherin MFI in both cell lines upon IRAK-1 &-4 dual inhibitor treatment **(Figure 5.22 E)**.

Flow cytometric analysis indicated 22.3 ± 3.2 % Vimentin+ cells in the chemo-resistant cell line. This was 1.8-fold more compared to the levels of Vimentin+ cells in parent HEp-2 (12.2 ± 4.5 %) **(Figure 5.22 D)**. The data is represented as histograms in **Figure 5.22 B**. Treatment with IRAK-1 &-4 dual inhibitor also suppressed the percentage of Vimentin+ chemo-resistant cells which became equivalent to the percentage of Vimentin+ cells in parent HEp-2 **(Figure 5.22 D)**. A significant decrease in Vimentin MFI was also observed in chemo-resistant HEp-2 upon IRAK-1 &-4 dual inhibitor treatment **(Figure 5.22 E)**. The data is represented as histograms in **Figure 5.22 C**.

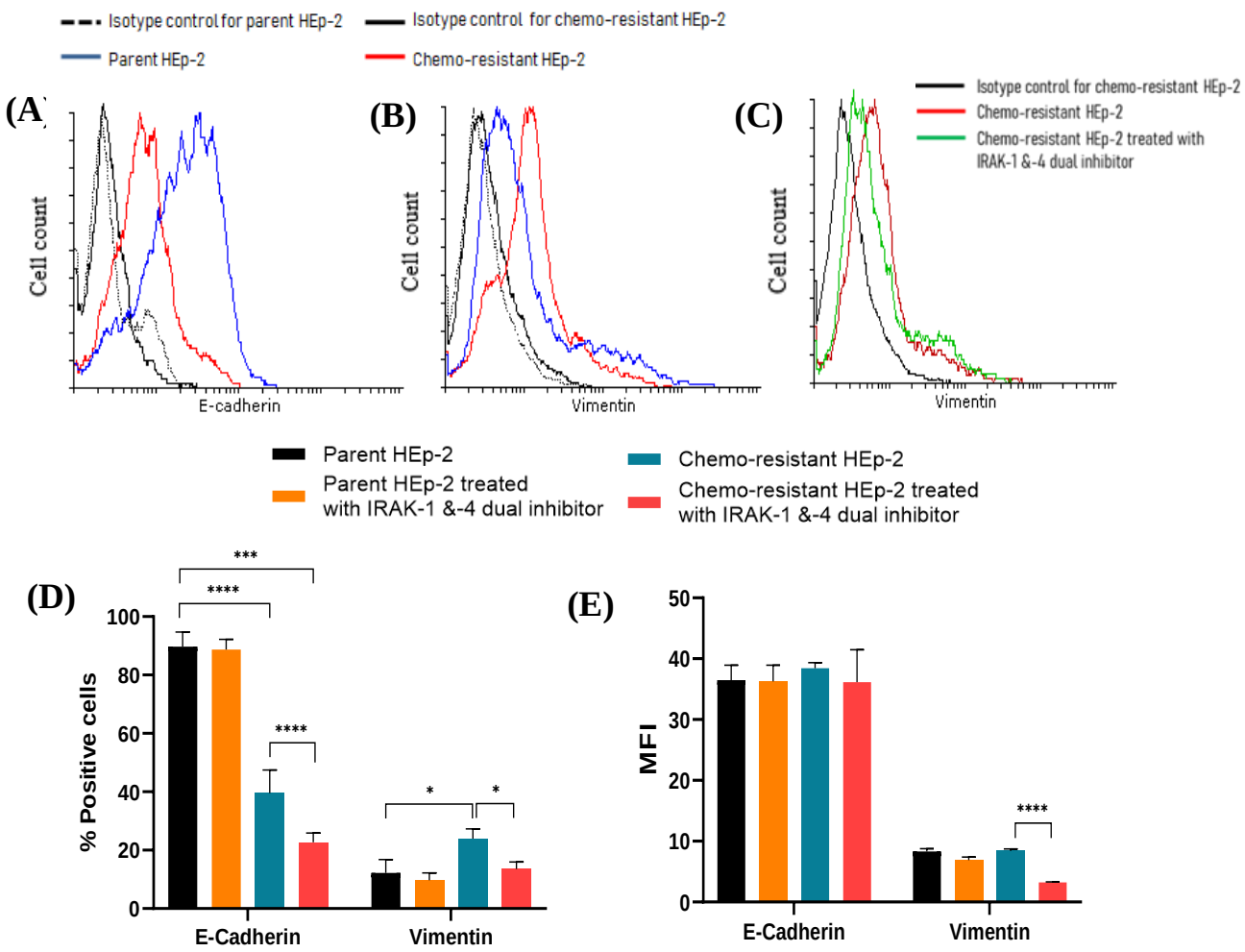

Figure 5.22: Effect of inhibition of the TLR signaling pathway on the EMT of chemo-resistant HEp-2 cell line. (A) Representative flow cytometric histogram image for E-cadherin expression in parent and chemo-resistant HEp-2. (B) Representative flow cytometric histogram image for Vimentin expression in parent and chemo-resistant HEp-2. (C) Representative flow cytometric histogram image for Vimentin expression in IRAK-1 &-4 dual inhibitor treated chemo-resistant HEp-2. (D) Bar graph of percentage of E-cadherin+ and Vimentin+ cells in chemo-resistant and parent HEp-2 with and without IRAK-1 &-4 dual inhibitor treatment determined by flow cytometry. (E) Bar graph of E-cadherin and Vimentin MFI in chemo-resistant and parent HEp-2 with and without IRAK-1 &-4 dual inhibitor treatment determined by flow cytometry Data from three independent experiments is summarized and presented as mean ± S.D. (*p<0.05, ***p<0.001, ****p<0.0001)

5.4.7.5 Impact of TLR signaling on the metastasis of chemo-resistant HNSCC cell line

The metastatic potential of the chemo-resistant cell line was determined by evaluating the mRNA expression of *MMP-2* and secretion of IL-6 from cells by ELISA.

MMP-2 expression was observed in chemo-resistant HEp-2 with a C_t value of 23.73±0.46. There was a 12-fold increase in the mRNA expression of *MMP-2* in the chemo-resistant cells compared to the parent cells. Treatment with IRAK-1 &-4 dual inhibitor significantly decreased the *MMP-2* mRNA expression by 9-fold in chemo-resistant HEp-2 (C_t=29.97±0.37). Of the two cell lines, IRAK-1 &-4 dual inhibitor treatment effectively suppressed the mRNA expression of *MMP-2* in the chemo-resistant cell line only **(Figure 5.23 A)**.

High IL-6 secretion was observed from the chemo-resistant cells (3087.33 ± 114.5 pg/mL). A strong reduction in these levels in the chemo-resistant HEp-2 by 2317 ± 56.26 pg/mL were observed following IRAK-1 &-4 dual inhibitor treatment. These levels were also drastically lower than IL-6 levels quantitated in the parent cell line **(Figure 5.23 B)**.

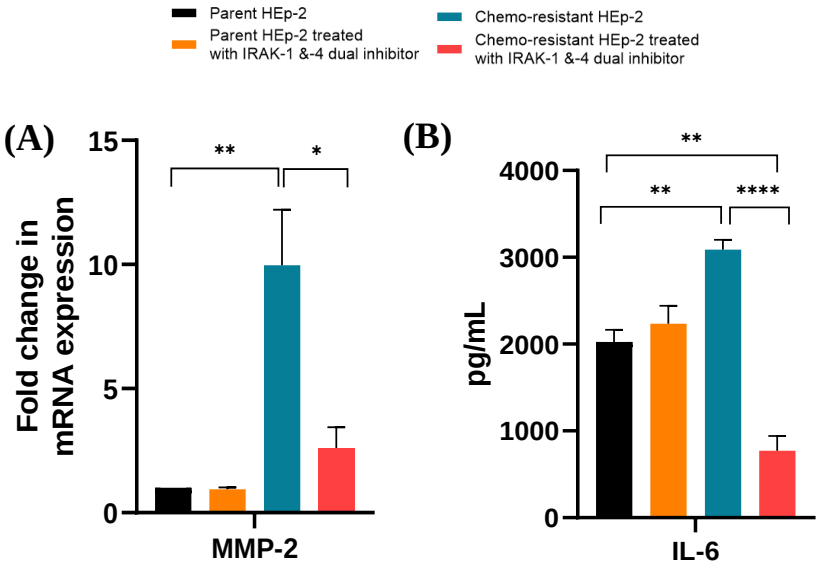

Figure 5.23: Effect of inhibition of the TLR signaling pathway on metastasis of chemo-resistant HEp-2 cell line. (A) Bar graph of fold expression of *MMP-2* in chemo-resistant compared to parent HEp-2 with and without treatment of IRAK-1 &-4 dual inhibitor. (B) Bar graph of IL-6 levels in chemo-resistant HEp-2 compared to parent HEp-2 with and without treatment of IRAK-1 &-4 dual inhibitor. Data from three independent experiments is summarized and presented as mean ± S.D. (*p<0.05, **p<0.01, ****p<0.0001).

5.5 Evaluation of therapeutic potential of TLR signaling inhibitor as combination therapy with conventional chemo-drugs using HNSCC cell line

The therapeutic potential of inhibiting the TLR signaling using IRAK-1 &-4 dual inhibitor in combination with chemo-drugs docetaxel, cisplatin and 5-FU was evaluated.

5.5.1 Effect of TLR signaling inhibitor-based combination therapy on cell viability of parent and chemo-resistant HNSCC cell lines

Viability of parent and chemo-resistant HEp-2 cells upon TLR inhibition in combination with individual chemo-drugs was determined by resazurin assay. Cells were treated with various concentration of chemo-drugs in combination with a single constant dose of IC_{25} of IRAK-1 &-4 dual inhibitor.

5.5.1.1 Effect of TLR signaling inhibitor and docetaxel-based combination therapy on the cell viability of parent and chemo-resistant HNSCC cell lines

IRAK-1 &-4 dual inhibitor combined with various concentrations of docetaxel suppressed the viability of both, parent and chemo-resistant HEp-2 **(Figure 5.24 A & B)**. The combination treatment significantly reduced the IC_{50} of docetaxel by 1.3-fold in parent and 207-fold in chemo-resistant HEp-2. A Comparative analysis of IC_{50} values of docetaxel, alone and in combination with IRAK-1 &-4 dual inhibitor on parent and chemo-resistant HEp-2 is presented in **Table 5.6**.

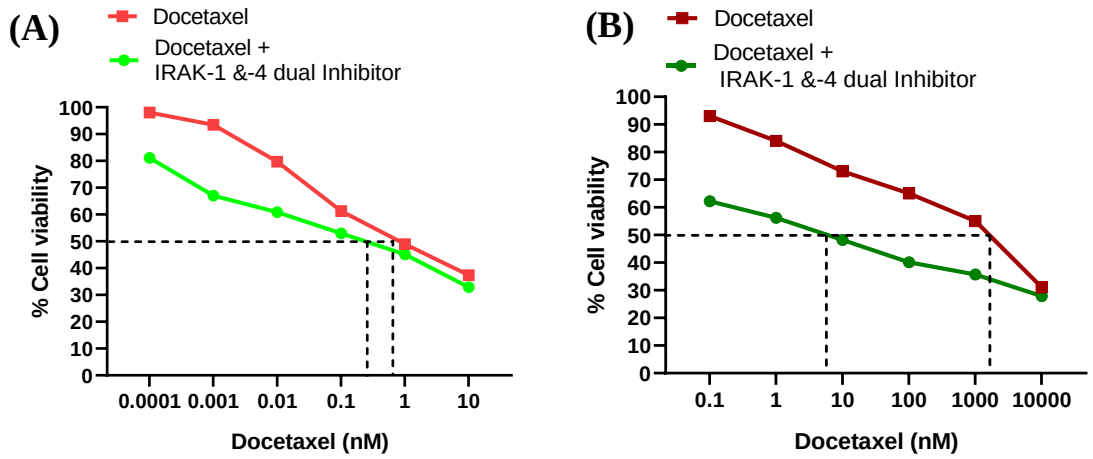

Figure 5.24: Effect of combination treatment of docetaxel and IRAK-1 &-4 dual inhibitor on the viability of parent and chemo-resistant HEp-2 cell lines. Viability of cells measured by resazurin assay upon combination treatment with docetaxel and IRAK-1 &-4 dual inhibitor on (A) parent HEp-2 and (B) chemo-resistant HEp-2. Percent cell viability curves for each treatment from one of the three independent experiments as a representative image is shown.

Table 5.6: Comparison of IC_{50} values of docetaxel alone and in combination with IRAK-1 &-4 dual inhibitor

Cell line	IC_{50} of docetaxel (n=6)	IC_{50} of docetaxel + IRAK-1 &-4 dual inhibitor (n=3)	% Decrease in IC_{50}	Fold decrease in IC_{50}
Parent HEp-2	0.864 ± 0.42 nM	0.63 ± 0.19 nM	27	1.3
Chemo-resistant HEp-2	1450 ± 0.7 nM	7.65 ± 0.68 nM	99.5	207

5.5.1.2 Effect of TLR signaling inhibitor and cisplatin-based combination therapy on the cell viability of parent and chemo-resistant HNSCC cell lines

IRAK-1 &-4 dual inhibitor combined with various concentrations of cisplatin suppressed the viability of both parent and chemo-resistant HEp-2 **(Figure 5.25 A & B)**. The combination treatment significantly reduced the IC_{50} of cisplatin by 1.4-fold in parent and 2.1-fold in chemo-resistant HEp-2. A Comparative analysis of IC_{50} values of cisplatin, alone and in combination with IRAK-1 &-4 dual inhibitor on parent and chemo-resistant HEp-2 is presented in **Table 5.7**.

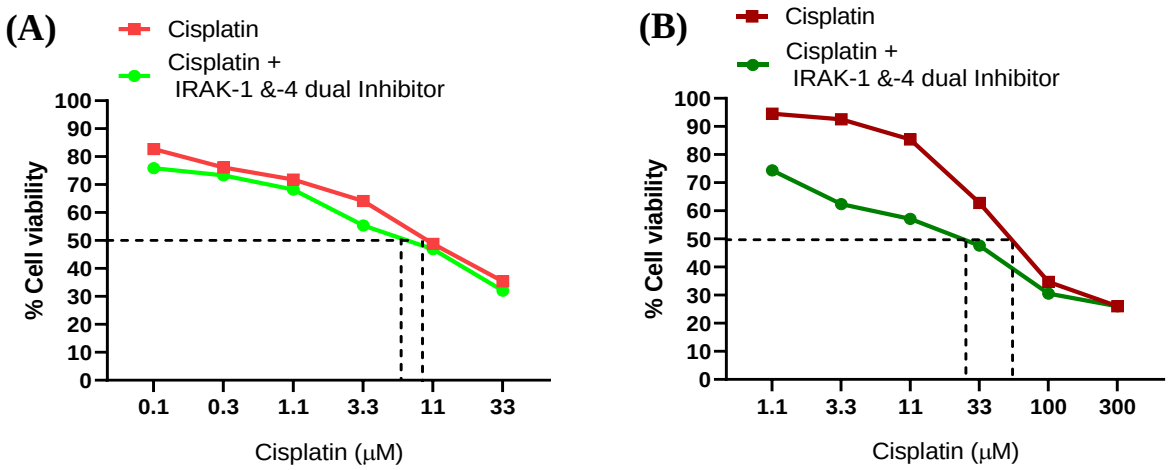

Figure 5.25: Effect of combination treatment of cisplatin and IRAK-1 &-4 dual inhibitor on the viability of parent and chemo-resistant HEp-2 cell lines. Viability of cells measured by resazurin assay upon combination treatment with cisplatin and IRAK-1 &-4 dual inhibitor on (A) parent HEp-2 and (B) chemo-resistant HEp-2. Percent cell viability curves for each treatment from one of the three independent experiments as a representative image is shown.

Table 5.7: Comparison of IC_{50} values of cisplatin alone and in combination with IRAK-1 &-4 dual inhibitor

Cell line	IC_{50} of cisplatin (n=6)	IC_{50} of cisplatin + IRAK-1 &-4 dual inhibitor (n=3)	% Decrease in IC_{50}	Fold decrease in IC_{50}
Parent HEp-2	9.73 ± 2.5 µM	6.8 ± 2.73 µM	30.11	1.4
Chemo-resistant HEp-2	53.04 ± 4.88 µM	25.2 ± 5 µM	52.48	2.10

5.5.1.3 Effect of TLR signaling inhibitor and 5-FU based combination therapy on the cell viability of parent and chemo-resistant HNSCC cell lines

IRAK-1 &-4 dual inhibitor combined with various concentrations of 5-FU suppressed the viability of both parent and chemo-resistant HEp-2 **(Figure 5.26 A & B)**. The combination treatment significantly reduced the IC_{50} of 5-FU by 1.9-fold in parent and 6.2-fold in chemo-resistant HEp-2. A Comparative analysis of IC_{50} values of 5-FU, alone and in combination with IRAK-1 &-4 dual inhibitor on parent and chemo-resistant HEp-2 is presented in **Table 5.8**.

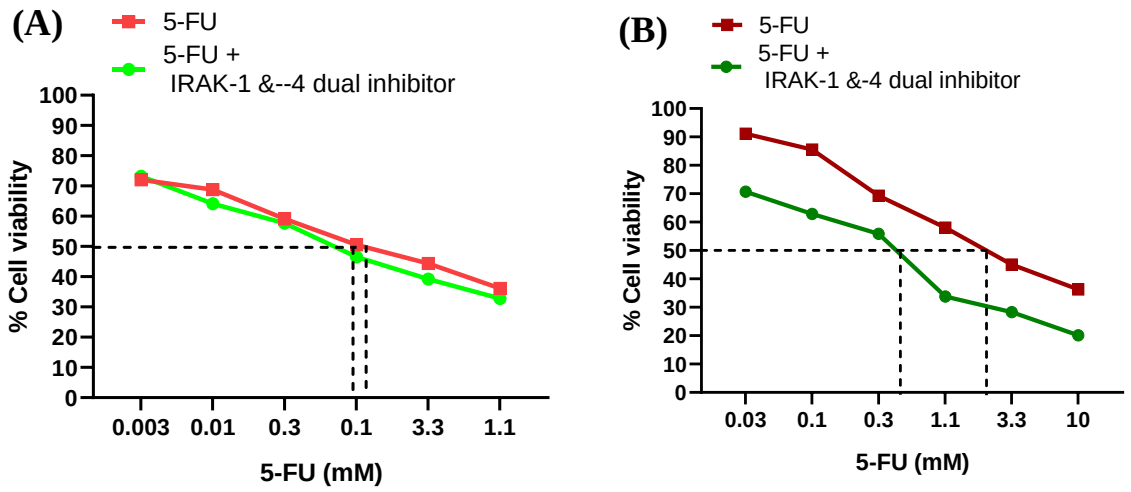

Figure 5.26: Effect of combination treatment of 5-FU and IRAK-1 &-4 dual inhibitor on the viability of parent and chemo-resistant HEp-2 cell line. Viability of cells measured by resazurin assay upon combination treatment with 5-FU and IRAK-1 &-4 dual inhibitor on (A) parent HEp-2 and (B) chemo-resistant HEp-2. Percent cell viability curves for each treatment from one of the three independent experiments as a representative image is shown.

Table 5.8: Comparison of IC_{50} values of 5-FU alone and in combination with IRAK-1 &-4 dual inhibitor

Cell line	IC_{50} of 5-FU (n=6)	IC_{50} of 5-FU + IRAK-1 &-4 dual inhibitor (n=3)	% Decrease in IC_{50}	Fold decrease in IC_{50}
Parent HEp-2	0.286 ± 0.84 mM	0.151 ± 0.04 mM	47.2	1.9
Chemo-resistant HEp-2	2.8 ± 0.8 mM	0.45 ± 0.42 mM	83.92	6.2

5.5.2 Effect of TLR signaling inhibitor-based combination therapy on survival of chemo-resistant HNSCC cell line

Treating the chemo-resistant cell line with TLR signaling inhibitor alone, led to significant downregulation of *Bcl-2* and *Bcl-xL* mRNA levels. Interestingly, a robust significant increase in the mRNA levels of *Bcl-2* and *Bcl-xL* was observed upon treatment with docetaxel, cisplatin and 5-FU at both the tested concentrations ranging between 5 to as high as approximately 100-350 folds increase. Among all the tested chemo-drugs, 5-FU showed maximum upregulation. The mRNA levels of *Bcl-2* were more elevated at $IC_{12.5}$ of docetaxel and 5-FU as compared to their IC_{25} doses while equivalent *Bcl-2* upregulation was observed for cisplatin irrespective of doses **(Figure 5.27 A)**. Similarly, the $IC_{12.5}$ of cisplatin and 5-FU induced higher mRNA levels of *Bcl-xL* than IC_{25} of the either chemo drug whereas the mRNA levels of *Bcl-xL* at both concentrations of docetaxel remained equal **(Figure 5.27 B)**. This indicated that chemo-drug exposure itself can trigger a stronger survival signaling through *Bcl-2* and *Bcl-xL* in the chemo-resistant cell line.

The combination treatment of constant dose of IRAK-1 &-4 dual inhibitor (IC_{25}) along with the respective doses of chemo-drugs significantly reduced the levels of *Bcl-2* mRNA. Docetaxel at higher doses completely abolished the expression of *Bcl-2* mRNA upon combining with IRAK-1 &-4 dual inhibitor while cisplatin seems to be effective in combination to bring down the levels of *Bcl-2* mRNA even lower than untreated chemo resistant line. Combining IRAK-1 &-4 dual inhibitor with 5-FU although significantly reduced the level of *Bcl-2* as compared to 5-FU as standalone therapy but could not reduce it to the extent similar to basal levels present in chemo resistant line without any treatment **(Figure 5.27 A)**.

Significantly reduced *Bcl-xL* mRNA levels were observed on combining the IRAK-1 &-4 dual inhibitor with individual chemo-drugs. The levels of *Bcl-xL* after the treatment with IRAK-1 &-4 dual inhibitor with both concentrations of docetaxel were similar to the levels of *Bcl-xL* in the untreated chemo-resistant cell. Combining IRAK-1 &-4 dual inhibitor with $IC_{12.5}$ of cisplatin reduced the mRNA levels of *Bcl-xL* compared to cisplatin alone although treatment of IC_{25} of cisplatin and IRAK-1 &-4 dual inhibitor provided a better overall response as *Bcl-xL* mRNA levels could not be detected at this combination. Combining IRAK-1 &-4 dual inhibitor with 5-FU also significantly reduced the mRNA levels of *Bcl-xL* compared to 5-FU monotherapy **(Figure 5.27 B)**.

Overall combining the chemo drug with IRAK-1 &-4 dual inhibitor resulted in significant reduction in cell survival related proteins' i.e., *Bcl-2* and *Bcl-xL* mRNA level.

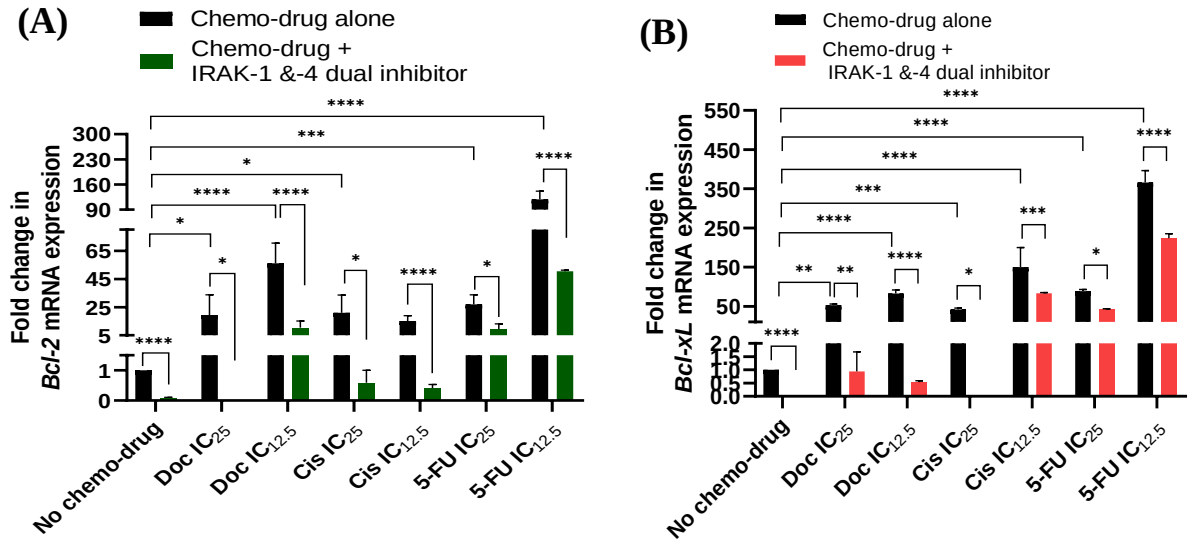

Figure 5.27: Effect of combination treatment of individual chemo-drugs and IRAK-1 &-4 dual inhibitor on the mRNA fold expression of *Bcl-2* and *Bcl-xL* of chemo-resistant HEp-2 cell line
(A) Bar graph of mRNA fold expression of *Bcl-2* upon single-drug and combination treatment. (B) Bar graph of mRNA fold expression of *Bcl-xL* upon single-drug and combination treatment. Data from three independent experiments is summarized and presented as mean ± S.D. (*p<0.05, **p<0.01, ***p<0.001, ****p<0.0001)

5.5.3 Effect of TLR signaling inhibitor-based combination therapy on the proliferative potential of parent and chemo-resistant HNSCC cell lines

The proliferative potential of parent and chemo-resistant HEp-2, upon inhibiting TLR signaling along with chemo-drugs therapy was evaluated by determining the expression of Ki-67.

Effect on parent HEp-2: A 30% rise in Ki-67+ cells was observed in the parent line on therapy with docetaxel at both concentrations and at IC_{25} of cisplatin. Inhibiting TLR signaling along with docetaxel and cisplatin treatment at IC_{25} reduced the percent of Ki-67+ cells compared to corresponding monotherapy. No significant alteration in Ki-67+ cells were observed on combination treatment with IRAK-1 &-4 dual inhibitor at the $IC_{12.5}$ of either docetaxel or cisplatin or at any dose of 5-FU. **Figure 5.28 A** shows the representative histograms demonstrating the effect of combination treatment on the Ki-67 expression in parent cells. **Figure 5.29 A** shows the effect of combination treatment on the percentage of Ki-67+ cells in parent HEp-2.

Effect on chemo-resistant HEp-2: The levels of Ki-67+ cells at IC_{25} of docetaxel remained unchanged, but a marginal increase in the levels were observed at $IC_{12.5}$ in the chemo-resistant line. Treatment with cisplatin at IC_{25} alone resulted in a 20% rise in the Ki-67+ cells in the resistant line, which was also the maximum rise observed among all chemo drug treatments. Contrasting to these observations, standalone therapy with 5-FU at both concentrations, reduced the percent of Ki-67+ cells in chemo-resistant line by 10%. After combining IRAK-1 &-4 dual inhibitor, minimal reductions in levels of Ki-67+ cells were observed with IC_{25} of cisplatin but were equivalent to those of the untreated resistant cell line with $IC_{12.5}$ of docetaxel and cisplatin. The combination treatment with docetaxel at IC_{25} or with 5-FU at any dose did not alter the Ki-67+ cells. **Figure 5.28 B** shows the representative histograms demonstrating the effect of combination treatment on the Ki-67 expression in chemo-resistant cells. **Figure 5.29 B** shows the effect of combination treatment on the percentage of Ki-67+ cells in chemo-resistant HEp-2.

The data indicates that chemotherapy with docetaxel and cisplatin itself can increase the proliferative potential of both parent and chemo-resistant HNSCC cells. 5-FU therapy does not affect the parent cell's proliferative potential but can inhibit that of resistant HNSCC cells. Inhibiting TLR signaling along with docetaxel and cisplatin therapy decreases the proliferative potential of both parent and resistant HNSCC cells.

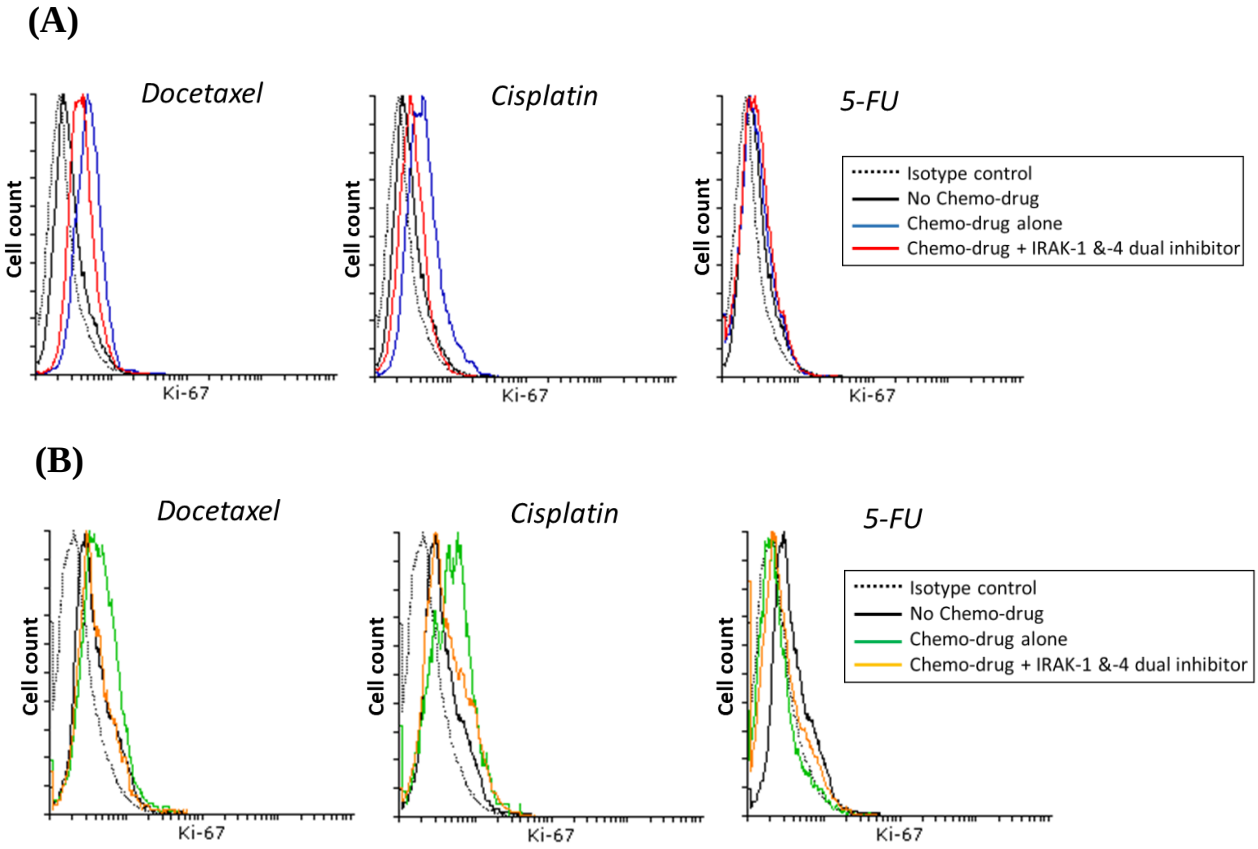

Figure 5.28: Representative histogram images demonstrating the effect of combination treatment of individual chemo-drugs and IRAK-1 &-4 dual inhibitor on the Ki-67 expression of parent and chemo-resistant HEp-2 cell lines. (A) Representative flow cytometric histogram images demonstrating the effect of combination treatment on Ki-67 expression in parent cells. (B) Representative flow cytometric histogram images demonstrating the effect of combination treatment on Ki-67 expression in chemo-resistant cells.

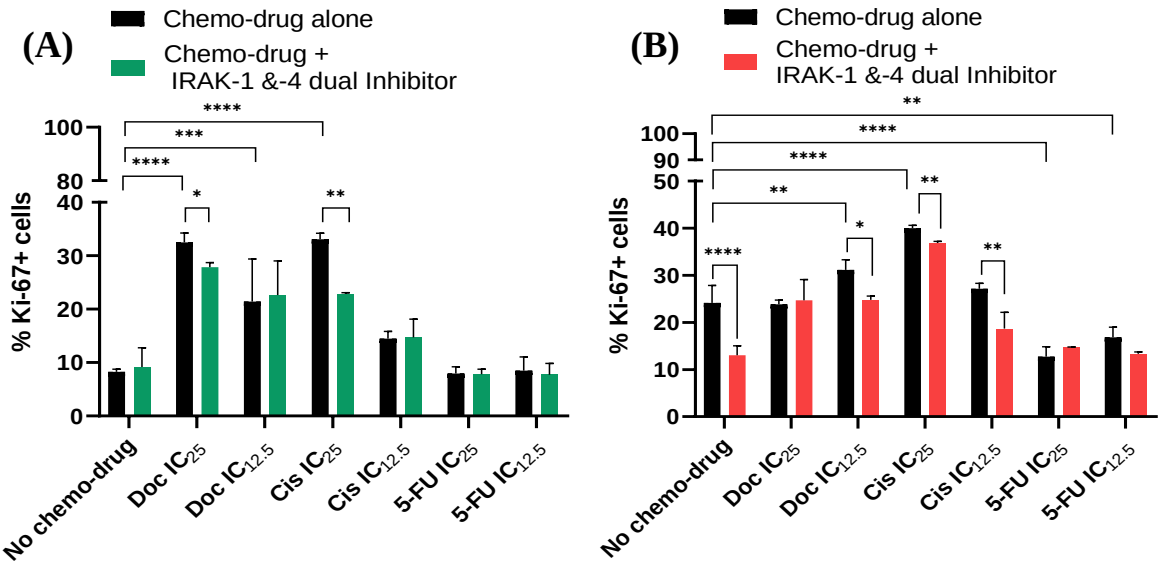

Figure 5.29: Effect of combination treatment of individual chemo-drugs and IRAK-1 &-4 dual inhibitor on the Ki-67 expression of parent and chemo-resistant HEp-2 cell lines. (A) Bar graph of percentage of Ki-67+ cells upon single-drug and combination treatment in parent HEp-2. (B) Bar graph of percentage of Ki-67+ cells upon single-drug and combination treatment in chemo-resistant HEp-2. Data from three independent experiments is summarized and presented as mean ± S.D. (*p<0.05, **p<0.01, ****p<0.0001)

5.5.4 Effect of TLR signaling inhibitor-based combination therapy on the CSCs of parent and chemo-resistant HNSCC cell lines

Expression of CSCs markers CD44 and Nanog in parent and chemo-resistant HEp-2, upon TLR inhibition in combination with the conventional chemo-drugs was evaluated. Expression of CSCs marker ALDH1 in chemo resistant HEp-2 upon combination treatment was also evaluated.

5.5.4.1 Effect of TLR signaling inhibitor-based combination therapy on the CD44 expression of parent and chemo-resistant HNSCC cell lines

Effect on parent HEp-2: Docetaxel treatment significantly upregulated CD44+ cells by 10 % in the parent cells. A similar rise in CD44+ cells was also observed on treating cells with IC_{25} of cisplatin. The level of CD44+ cells at treatment with $IC_{12.5}$ of cisplatin and 5-FU at both doses remained unchanged. Combining IRAK-1 &-4 dual inhibitor with the individual chemo-drugs did not demonstrate any change in the percentage of CD44+ cells in parent HEp-2. **Figure 5.30 A** shows the representative histograms demonstrating the effect of combination treatment on the CD44 expression in parent cells. **Figure 5.31 A** shows the effect of combination treatment on the percentage of CD44+ cells in parent HEp-2.

Effect on chemo-resistant HEp-2: In the resistant cell line, the CD44+ cells were higher by 15 % compared to parent's. Standalone therapy with docetaxel marginally enhanced the CD44+ cells population in the resistant line. This increase was suppressed by combining IRAK-1 &-4 dual inhibitor with docetaxel. No change in CD44+ cells were observed upon cisplatin and 5-FU treatment or on combining the inhibitor with them. **Figure 5.30 B** shows the representative histograms demonstrating the effect of combination treatment on the CD44 expression in chemo-resistant cells. **Figure 5.31 B** shows the effect of combination treatment on the percentage of CD44+ cells in chemo-resistant HEp-2.

Data indicates that docetaxel and cisplatin exposure may amplify stemness in parent and chemo-resistant HNSCC cells by upregulating the levels of CD44. These levels can be reduced by inhibiting TLR signaling along with docetaxel therapy in resistant cells but the approach of inhibiting TLR signaling with chemo-drugs seems to be ineffective on the suppression of the levels of CD44 of parent line.

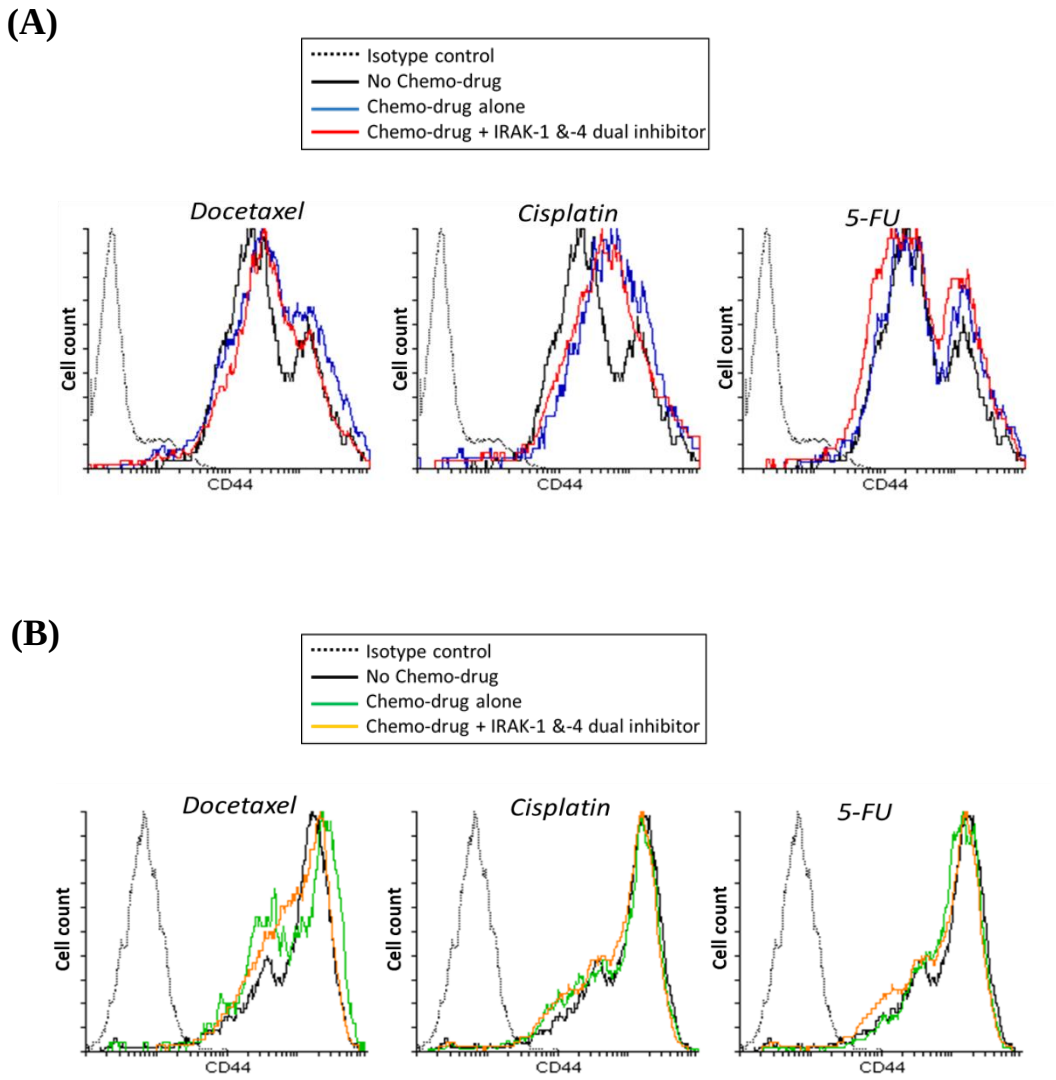

Figure 5.30: Representative histogram images demonstrating the effect of combination treatment of individual chemo-drugs and IRAK-1 &-4 dual inhibitor on the CD44 expression of parent and chemo-resistant HEp-2 cell lines. (A) Representative flow cytometric histogram images demonstrating the effect of combination treatment on CD44 expression in parent cells. (B) Representative flow cytometric histogram images demonstrating the effect of combination treatment on CD44 expression in chemo-resistant cells.

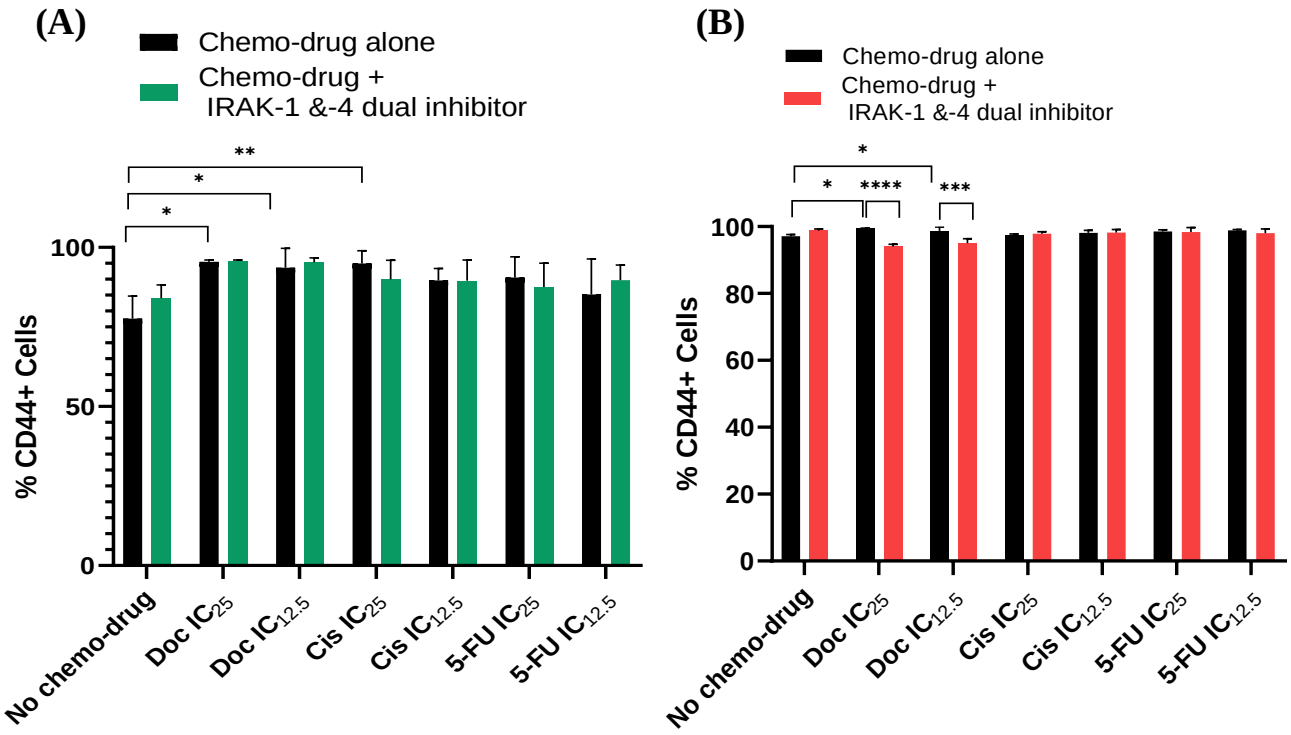

Figure 5.31: Effect of combination treatment of individual chemo-drugs and IRAK-1 &-4 dual inhibitor on the CD44 expression of parent and chemo-resistant HEp-2 cell lines. (A) Bar graph of percentage of CD44+ cells upon single-drug and combination treatment in parent HEp-2. (B) Bar graph of percentage of CD44+ cells upon single-drug and combination treatment in chemo-resistant HEp-2. Data from three independent experiments is summarized and presented as mean ± S.D. (*p<0.05, **p<0.01, ***p<0.001, ****p<0.0001)

5.5.4.2 Effect of TLR signaling inhibitor-based combination therapy on the Nanog expression of parent and chemo-resistant HNSCC cell lines

Effect on parent HEp-2: All three chemo-drugs treatment significantly elevated the Nanog+ cells population in parent cells by 20%, except $IC_{12.5}$ of cisplatin and 5-FU, where no significant change could be seen. IRAK-1 &-4 dual inhibitor combination at IC_{25} of docetaxel, but not at $IC_{12.5}$ significantly reduced the percentage of Nanog+ cells compared to standalone docetaxel treatment. Combining the inhibitor with the other chemo-drugs did not show any significant effect on the percentage of Nanog+ cells **Figure 5.32 A** shows the representative histograms demonstrating the effect of combination treatment on the Nanog expression in parent cells. **Figure 5.33 A** shows the effect of combination treatment on the percentage of Nanog+ cells in parent HEp-2.

Effect on chemo-resistant HEp-2: Significant elevations in levels of Nanog+ cells were observed in the resistant line as compared to parent line. Chemo-drugs treatment further enhanced these levels by 10%. Although, 5-FU treatment at IC_{25} did not show any change in the percent of Nanog+ cells, but $IC_{12.5}$ increased them marginally. Combining IRAK-1 &-4 dual inhibitor with the chemo-drugs exhibited significant reduction in the percent of Nanog+ cells as compared to chemo-drug therapy alone. The percent of Nanog+ cells on combination treatment of IRAK-1 &-4 dual inhibitor with docetaxel at IC_{25} and, with cisplatin and 5-FU at $IC_{12.5}$ were similar to those of parent's. Inhibitor treatment with $IC_{12.5}$ of docetaxel and IC_{25} of cisplatin also reduced Nanog+ cells population compared to the corresponding monotherapy. **Figure 5.32 B** shows the representative histograms demonstrating the effect of combination treatment on the Nanog expression in chemo-resistant cells. **Figure 5.33 B** shows the effect of combination treatment on the percentage of Nanog+ cells in chemo-resistant HEp-2.

Data suggests that chemo therapy can mediate Nanog upregulation, further enhancing the stemness of both parent and chemo resistant HNSCC cells. TLR inhibition along with chemo therapy may overcome stemness induced by Nanog over-expression in chemo-resistant HNSCC cells although the therapy does not show much effect in parent HNSCC cells.

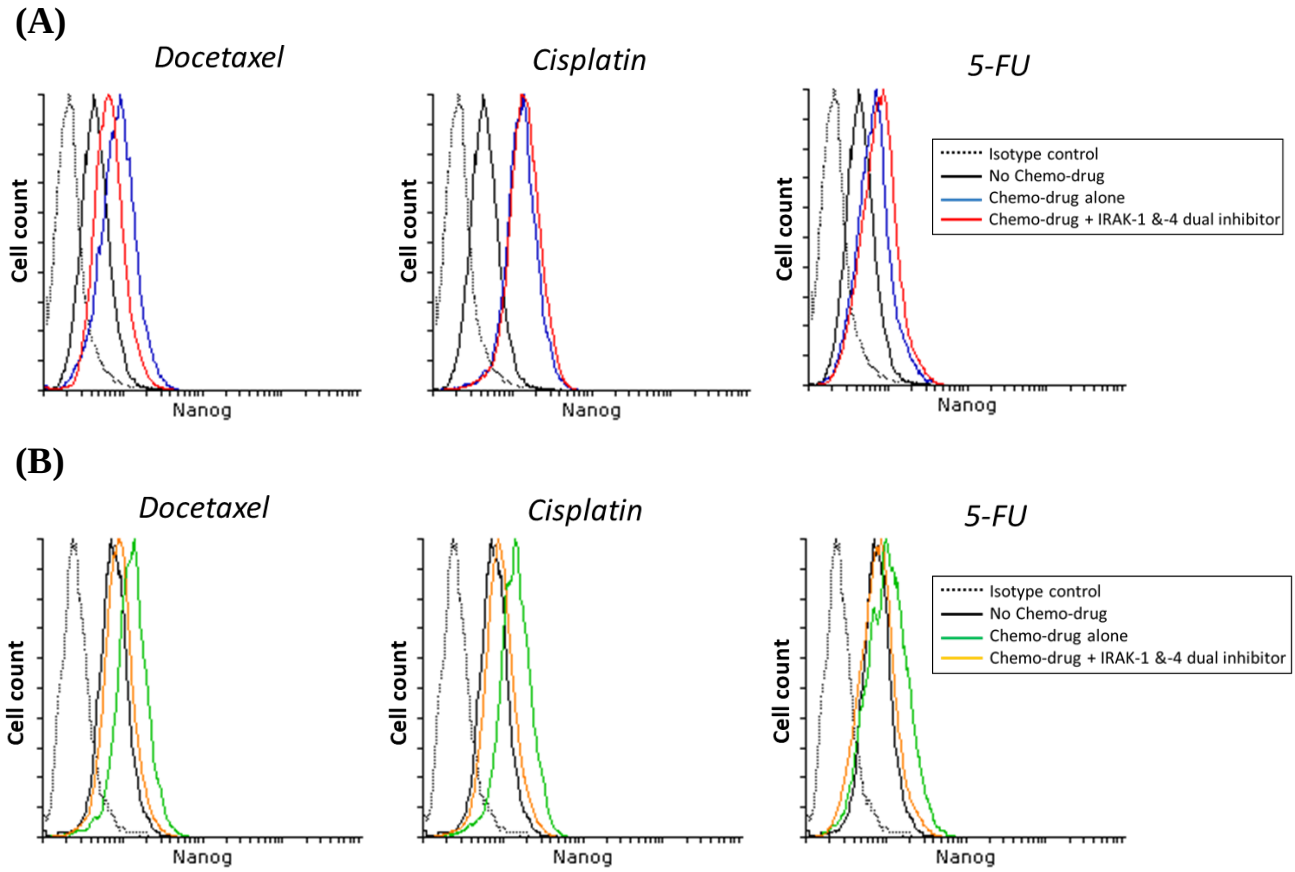

Figure 5.32: Representative histogram images demonstrating the effect of combination treatment of individual chemo-drugs and IRAK-1 &-4 dual inhibitor on the Nanog expression of parent and chemo-resistant HEp-2 cell lines. (A) Representative flow cytometric histogram images demonstrating the effect of combination treatment on Nanog expression in parent cells. (B) Representative flow cytometric histogram images demonstrating the effect of combination treatment on Nanog expression in chemo-resistant cells.

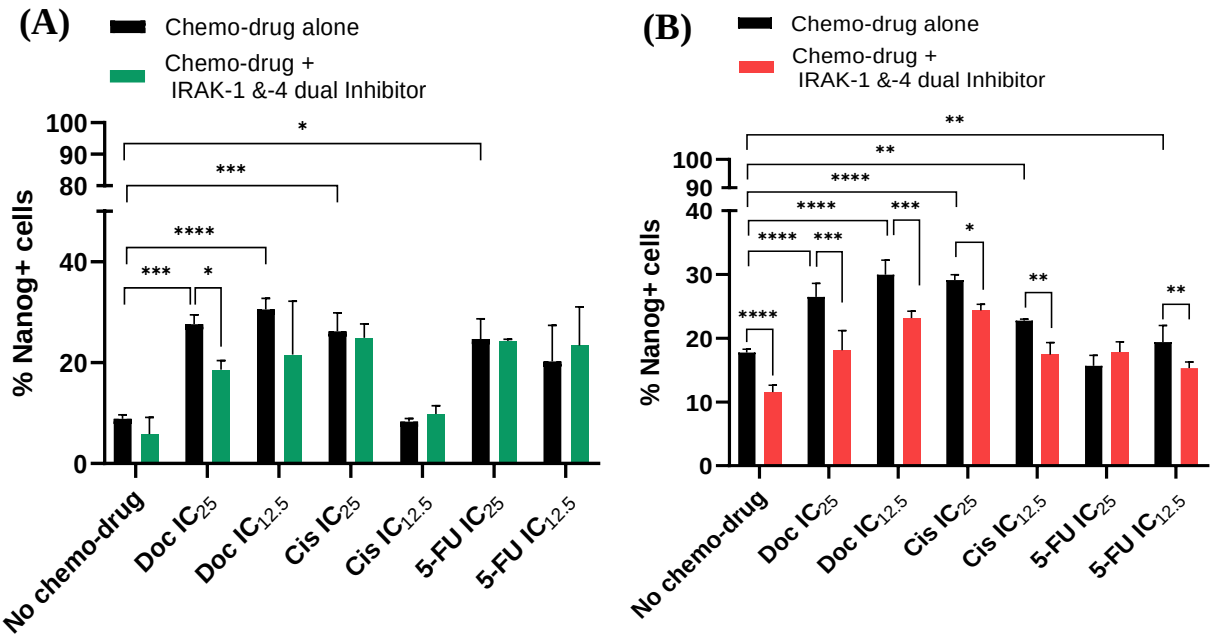

Figure 5.33: Effect of combination treatment of individual chemo-drugs and IRAK-1 &-4 dual inhibitor on the Nanog expression of parent and chemo-resistant HEp-2 cell lines. (A) Percentage of Nanog+ cells upon single-drug and combination treatment in parent HEp-2. (B) Percentage of Nanog+ cells upon single-drug and combination treatment in chemo-resistant HEp-2. Data from three independent experiments is summarized and presented as mean ± S.D. (*p<0.05, **p<0.01, ***p<0.001, ****p<0.0001)

5.5.4.3 Effect of TLR signaling inhibitor-based combination therapy on the ALDH1 expression of chemo-resistant HNSCC cell line

Since the combination therapy demonstrated a better response in reducing the stemness of the resistant cell line as compared to the parent cell line, we examined the expression of CSCs marker ALDH1 in the resistant cell line upon combination treatment by western blotting **(Figure 5.34 A)**. Stand-alone treatment with docetaxel and 5-FU reduced more than half of the ALDH1 expression in chemo-resistant cells. Treatment with cisplatin did not have any significant effect **(Figure 5.34 B)**.

No further reduction in the expression of ALDH1 was observed on combining IRAK-1 &-4 dual inhibitor with any of the chemo-drugs **(Figure 5.34 B)**. This data suggested that docetaxel and 5-FU treatment alone may reduce stemness in resistant HNSCC cells through ALDH1 reduction but TLR inhibition along with chemo therapy does not impact the ALDH1 expression in resistant HNSCC cells.

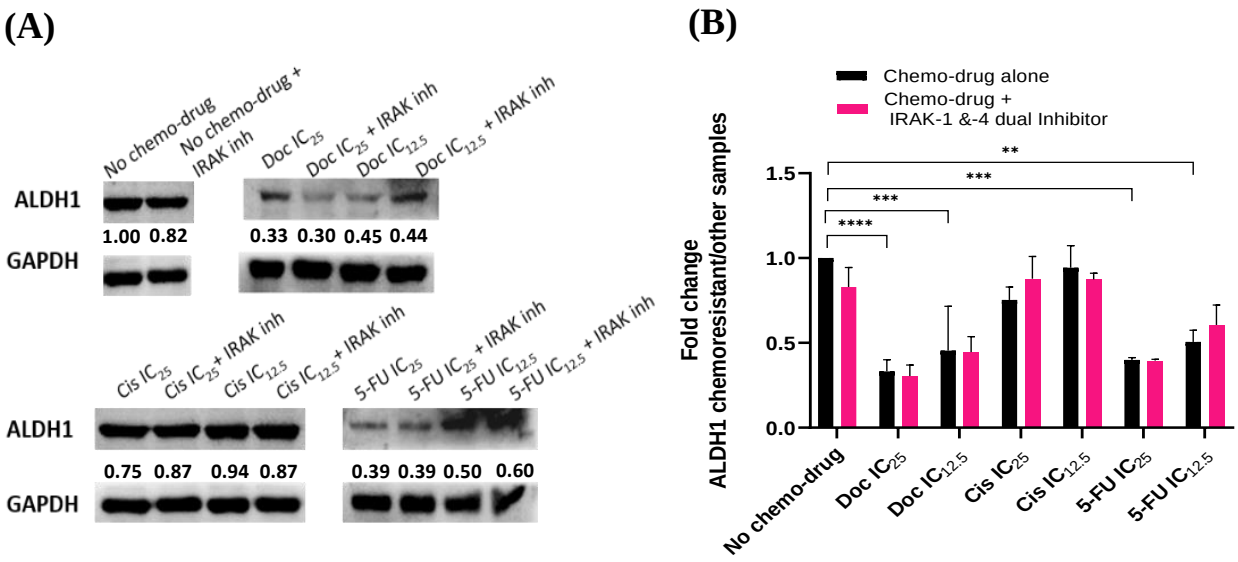

Figure 5.34: Effect of combination treatment of individual chemo-drugs and IRAK-1 &-4 dual inhibitor on the ALDH1 expression of chemo-resistant HEp-2 cell line. (A) Representative western blotting image demonstrating the effect of combination treatment on ALDH1 expression in cells. (B) Bar graph of fold change in ALDH1 expression upon single-drug and combination treatment. Data from three independent experiments is summarized and presented as mean ± S.D. (**p<0.01, ***p<0.001, ****p<0.0001).

5.5.5 Effect of TLR signaling inhibitor-based combination therapy on the EMT of chemo-resistant HNSCC cell line

To further understand the effect of TLR inhibition along with chemo therapy on the EMT of resistant HNSCC cells, E-cadherin and Vimentin levels were analyzed by flow cytometry.
The E-cadherin+ cells significantly increased by 10% when treated with IC_{25} of cisplatin, in the resistant cell line. The other chemo-drugs treatment could not alter the levels of E-cadherin. IRAK-1 &-4 dual inhibitor, when combined with IC_{25} of cisplatin and $IC_{12.5}$ of 5-FU also decreased E-cadherin+ cells by 20% and 30%, respectively in the resistant cell line. Except at these combinations, the other chemo-drugs combinations did not show any significant difference in levels of E-cadherin+ cells. **Figure 5.35 A** shows the representative histograms demonstrating the effect of combination treatment on the E-cadherin expression in chemo-resistant cells. **Figure 5.35 B** shows the effect of combination treatment on the percentage of E-cadherin+ cells in chemo-resistant HEp-2.

A rise by 15-20% was observed at therapy on IC_{25} of docetaxel and cisplatin in the resistant cell line. The lower dose, $IC_{12.5}$ of these chemo-drugs did not change the Vimentin levels of the cell line. Combining the inhibitor with IC_{25} of docetaxel and cisplatin, as well as $IC_{12.5}$ of 5-FU restored the chemo therapy mediated increased levels of Vimentin+ cells in the resistant cell line. But, the combination treatment of IRAK-1 &-4 dual inhibitor with $IC_{12.5}$ of docetaxel and cisplatin significantly reduced the levels of Vimentin+ cells that were much lower even in comparison to the basal levels present in the resistant cell line. A reduced Vimentin MFI was also observed on combining the inhibitor with IC_{25} of cisplatin. **Figure 5.36 A** shows the representative histograms demonstrating the effect of combination treatment on the Vimentin expression in chemo-resistant cells. **Figure 5.36 B-i & ii** shows the effect of combination treatment on the percentage of Vimentin+ cells and Vimentin MFI, respectively in chemo-resistant HEp-2.

An EMT is demonstrated by a loss of E-cadherin and an increase in Vimentin. Our results, hence suggested that cisplatin alone treatment may suppress EMT through E-cadherin upregulation but further combining TLR inhibitor does not produce the desirable results. Our results also suggest that upregulated Vimentin upon chemo drug exposure may contribute to an enhanced EMT state in the resistant cells and the inhibition of TLR signaling in this condition can significantly suppress the process.

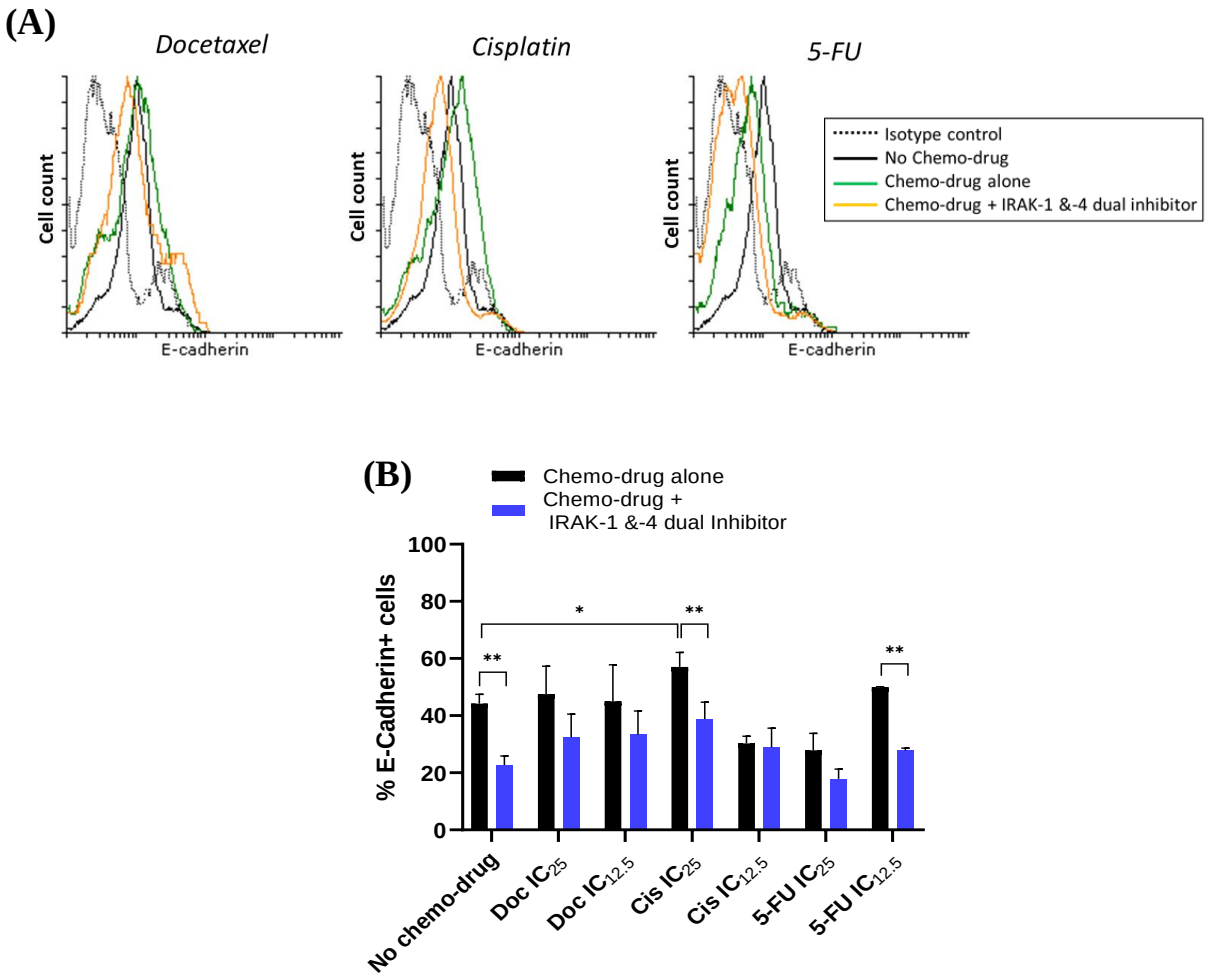

Figure 5.35: Effect of combination treatment of individual chemo-drugs and IRAK-1 &-4 dual inhibitor on the E-cadherin expression of chemo-resistant HEp-2 cell line. (A) Representative flow cytometric histogram images demonstrating the effect of combination treatment on E-cadherin expression in cells. (B) Bar graph of percentage of E-cadherin+ cells upon single-drug and combination treatment. Data from three independent experiments is summarized and presented as mean ± S.D. (*p<0.05, **p<0.01)

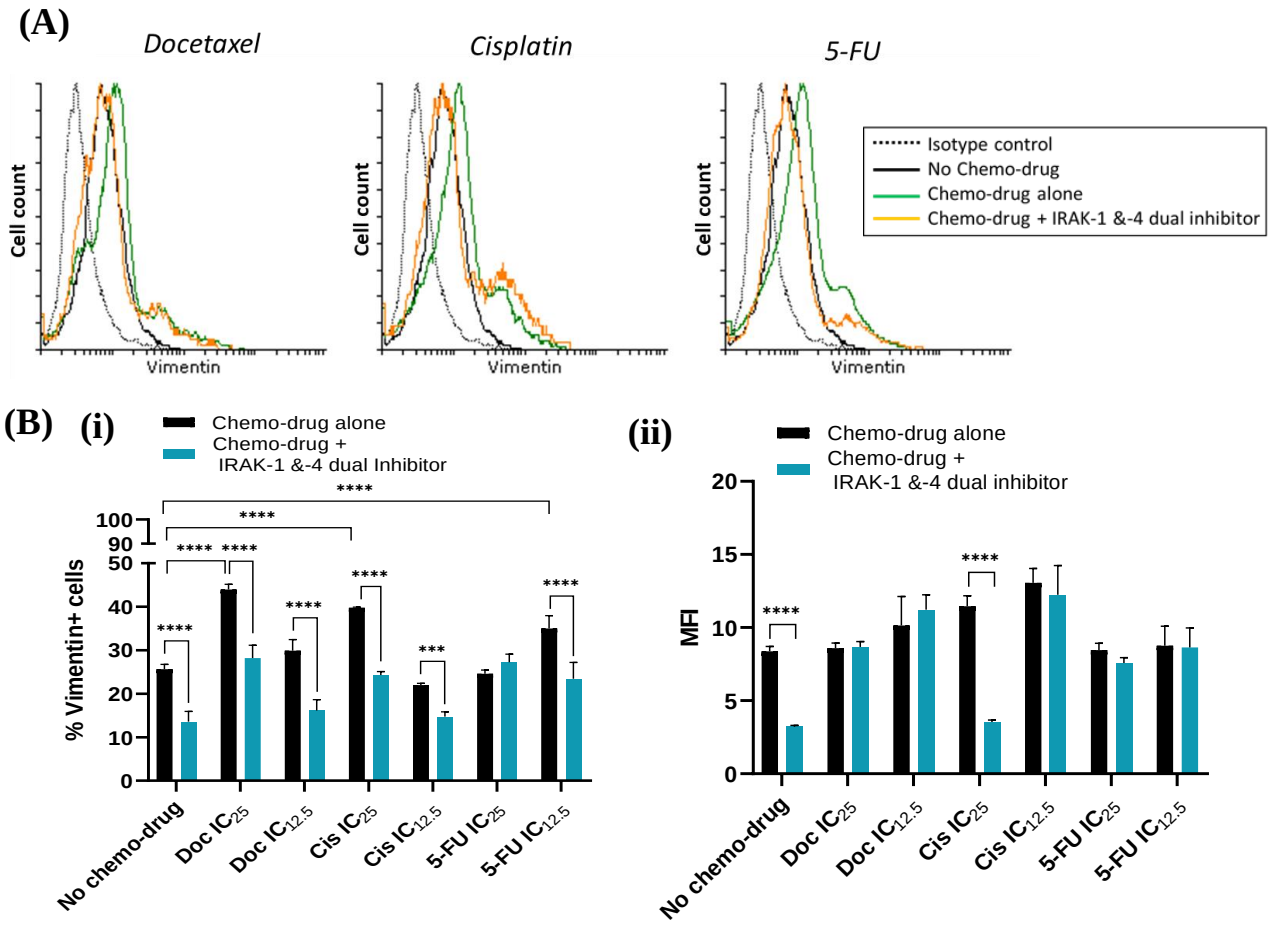

Figure 5.36: Effect of combination treatment of individual chemo-drugs and IRAK-1 &-4 dual inhibitor on the Vimentin expression of chemo-resistant HEp-2 cell line. (A) Representative flow cytometric histogram images demonstrating the effect of combination treatment on Vimentin expression in cells. (B) Bar graphs of (i) percentage of Vimentin+ cells and (ii) Vimentin MFI upon single-drug and combination treatment. Data from three independent experiments is summarized and presented as mean ± S.D. (***p<0.001, ****p<0.0001)

5.5.6 Effect of TLR signaling inhibitor-based combination therapy on the metastasis of chemo-resistant HNSCC cell line

The effect of TLR inhibition with chemo-drugs therapy on metastasis of chemo resistant HNSCC was examined by evaluating the expression of HNSCC specific metastasis markers MMP-2 and IL-6.

Chemotherapy led to a significant rise in mRNA levels of *MMP-2* in the resistant cell line. Cisplatin therapy at IC_{25} markedly induced the highest rise in the levels of *MMP-2* mRNA i.e., by 40-fold besides $IC_{12.5}$ of docetaxel and cisplatin, and IC_{25} of 5-FU, that also increased the *MMP-2* mRNA levels by 10-fold. Combining IRAK-1 &-4 dual inhibitor at these concentrations significantly reduced the mRNA levels of *MMP-2* in comparison of chemo drug alone therapy. Combination treatment of the TLR inhibitor with IC_{25} of 5-FU restored the levels of *MMP-2* mRNA in the resistant line. No significant changes in *MMP-2* mRNA level at IC_{25} of docetaxel and $IC_{12.5}$ of 5-FU at either alone or in combination with IRAK-1 &-4 dual inhibitor could be observed **(Figure 5.37 A)**.

ELISA analysis demonstrated a reduction in IL-6 levels upon treatment with all the three chemo-drugs, at all concentrations indicating the efficacy of chemo therapy alone. Combining IRAK-1 &-4 dual inhibitor along with docetaxel and cisplatin treatment further improved the efficacy of the chemo-drugs. A 1000-1500 pg/mL decrease in IL-6 levels were observed at combination treatment with IC_{25} of docetaxel and cisplatin, although at lower doses of these chemo-drugs, the reductions were marginal. Combination treatment of IRAK-1 &-4 dual inhibitor with 5-FU at any concentration did not yield any significant change in IL-6 levels **(Figure 5.37 B)**.

Our results indicate dual effect of chemo therapy on metastasis of resistant HNSCC cells. It promotes metastasis through MMP-2 upregulation whereas suppresses it through IL-6 degradation. But on inhibiting TLR signaling along with chemo therapy, the metastasis of resistant HNSCC cells is controlled through reduction of both cytokines, MMP-2 and IL-6.

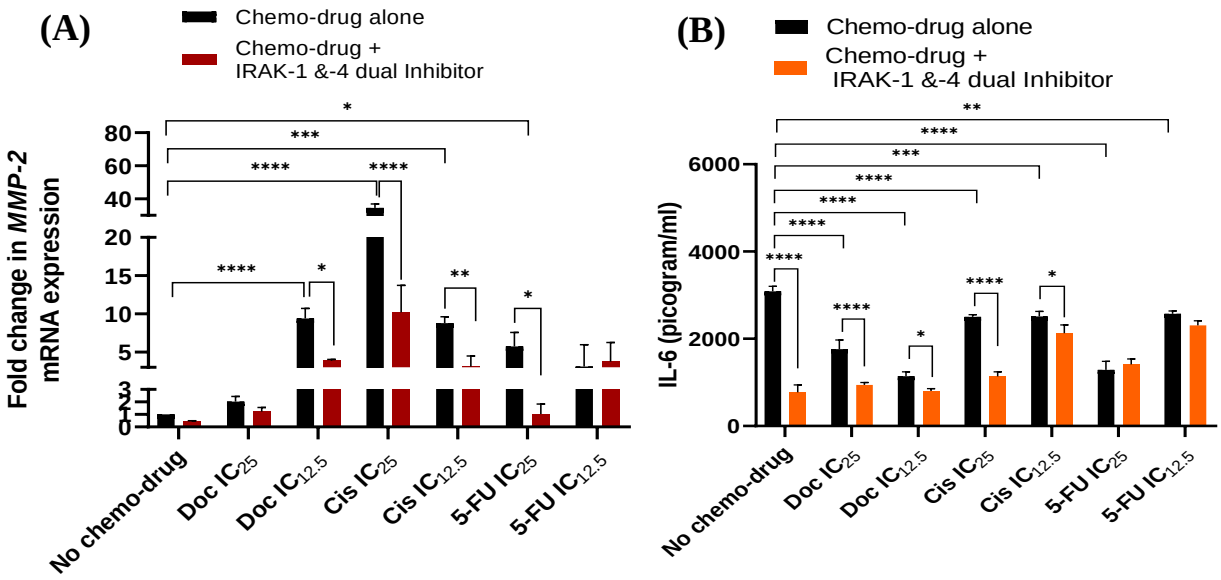

Figure 5.37: Effect of combination treatment of individual chemo-drugs and IRAK-1 &-4 dual inhibitor on the mRNA fold expression of *MMP-2* mRNA and IL-6 levels of chemo-resistant HEp-2 cell line. (A) Bar graph of mRNA fold expression of *MMP-2* upon single-drug and combination treatment. (B) Bar graph of IL-6 levels upon single-drug and combination treatment. Data from three independent experiments is summarized and presented as mean ± S.D. (*p<0.05, **p<0.01, ***p<0.001, ****p<0.0001)

5.5.7 Effect of TLR signaling inhibitor-based combination therapy on the BST-2 expression of parent and chemo-resistant HNSCC cell lines

BST-2 is reported to play a role in mediating resistant to gefitinib and cisplatin in HNSCC (Kuang *et al.*, 2017; Jin *et al.*, 2019). Our study also establishes an association of BST-2 with the CSCs in HNSCC. This suggest that regulating BST-2 levels in HNSCC can be therapeutically advantageous. Hence, we examined the effect of TLR inhibition with the chemo-drugs on the levels of BST-2 in the parent and resistant HNSCC cells.

Effect on parent HEp-2: The higher doses of cisplatin and 5-FU boosted the BST-2+ cells in the parent line. IC_{25} of cisplatin increased the levels of BST-2+ cells by 20%, while IC_{25} of 5-FU caused the highest rise in the levels of BST-2+ cells i.e., by 30%. At all combination treatment, the observed levels of BST-2+ cells were lower than those of the basal levels present in the resistant cell line, except at IC_{25} of 5-FU where the levels of BST-2 were lower that 5-FU alone treatment only. A significant reduction in BST-2 MFI at combination treatment of IRAK-1 &-4 dual inhibitor with IC_{25} of cisplatin and at both concentrations of 5-FU was observed. **Figure 5.38 A** shows the representative histograms demonstrating the effect of combination treatment on the BST-2 expression in parent cells. **Figure 5.39 A-i & ii** shows the effect of combination treatment on the percentage of BST-2+ cells and BST-2 MFI, respectively in parent HEp-2.

Effect on chemo-resistant HEp-2: In the resistant cell line, the chemo-drugs treatment did not affect the levels of BST-2. Combination treatment with $IC_{12.5}$ of docetaxel and IRAK-1 &-4 dual inhibitor reduced the levels by 20%. A marginal reduction in percent of BST-2+ cells was also found on combination treatment of $IC_{12.5}$ of cisplatin and IRAK-1 &-4 dual inhibitor. We also noted a robust reduction of 200 units in BST-2 MFI on docetaxel alone treatment at both concentrations in the resistant line although combining IRAK-1 &-4 dual inhibitor did not improve the effect further. IRAK-1 &-4 dual inhibitor with $IC_{12.5}$ of cisplatin and 5-FU also significantly reduced the BST-2 MFI in chemo-resistant HNSCC cells. **Figure 5.38 B** shows the representative histograms demonstrating the effect of combination treatment on the BST-2 expression in chemo-resistant cells. **Figure 5.39 B-i & ii** shows the effect of combination treatment on the percentage of BST-2+ cells and BST-2 MFI, respectively in chemo-resistant HEp-2.

These results suggested that inhibition of TLR signaling with chemo-drugs reduces the BST-2 levels of parent and resistant HNSCC cells, but the combination treatment has much better effect on parent cells compared to the resistant cells.

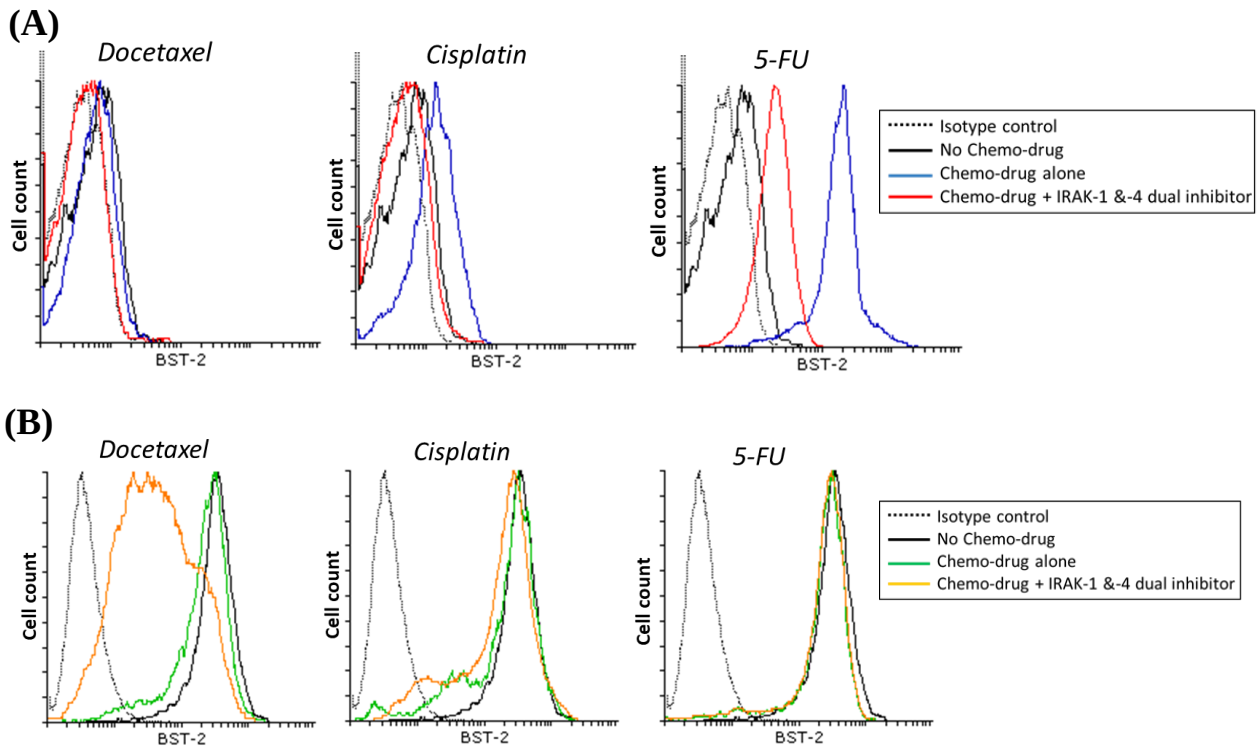

Figure 5.38: Representative histogram images showing the effect of combination treatment of individual chemo-drugs and IRAK-1 &-4 dual inhibitor on the BST-2 expression of parent and chemo-resistant HEp-2 cell lines. (A) Representative flow cytometric histogram images demonstrating the effect of combination treatment on BST-2 expression in parent cells. (B) Representative flow cytometric histogram images demonstrating the effect of combination treatment on BST-2 expression in chemo-resistant cells.

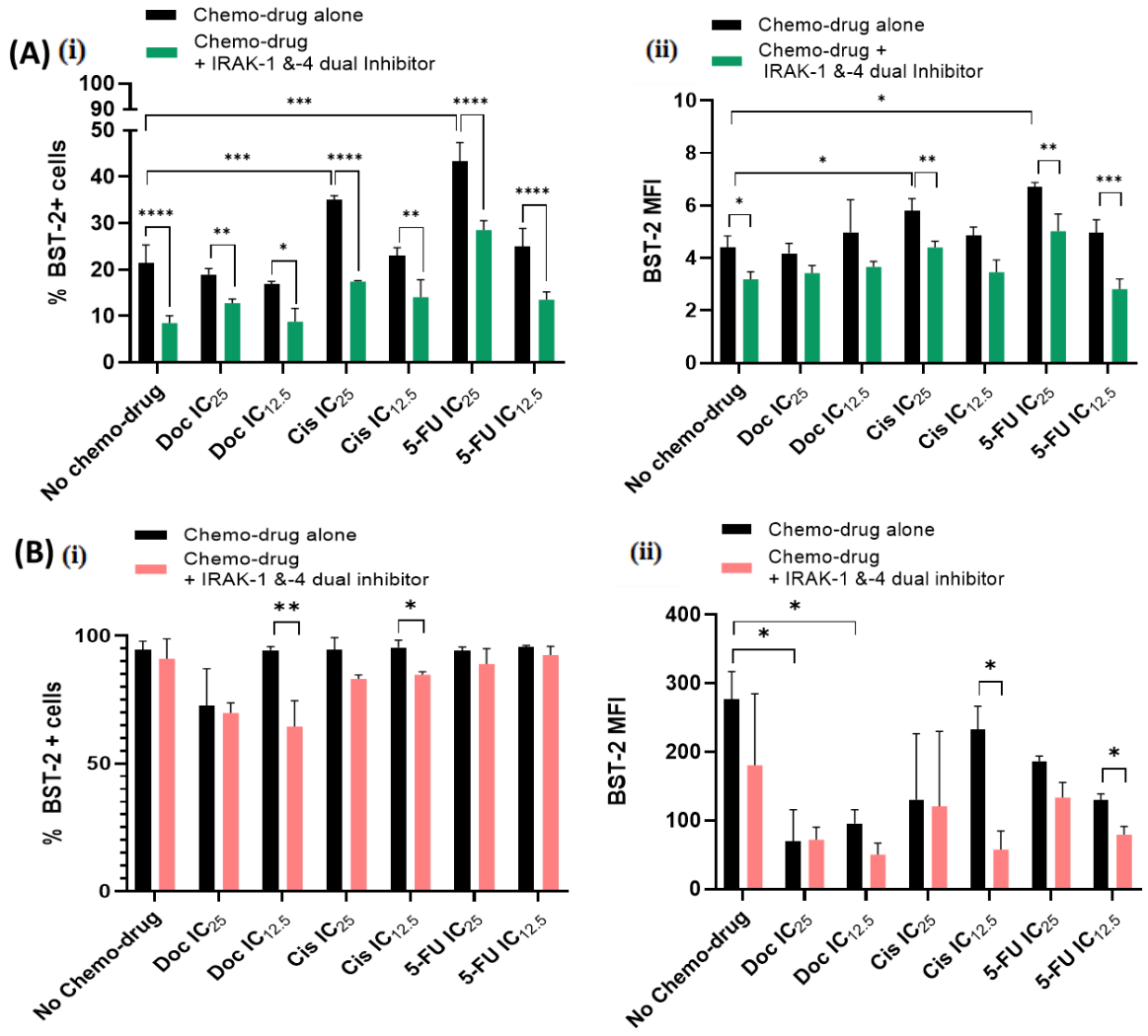

Figure 5.39: Effect of combination treatment of individual chemo-drugs and IRAK-1 &-4 dual inhibitor on the BST-2 expression of parent and chemo-resistant HEp-2 cell lines. (A) (i) Bar graph of percentage of BST-2+ cells and (ii) Bar graph of BST-2 MFI upon single-drug and combination treatment in parent HEp-2. (B) (i) Bar graph of percentage of BST-2+ cells and (ii) Bar graph of BST-2 MFI upon single-drug and combination treatment in chemo-resistant HEp-2. Data from three independent experiments is summarized and presented as mean ± S.D. (*p<0.05, **p<0.01, ***p<0.001, ****p<0.0001)